TAMPERE UNIVERSITY OF TECHNOLOGY

Faculty of Business and Built Environment
Department of Civil Engineering
Research Centre of Metal Structures

Kristo Mela, Hilkka Ronni, Markku Heinisuo

Comparative Evaluation of Steel Profiles in Roof Trusses

Topology Optimization and Structural Analysis

October 21, 2014

Contents

1 Introduction

The purpose of this document is to provide a comprehensive evaluation of different types of member profiles in roof trusses. Two groups of profiles are compared:

1. Chord profiles are HEA/HEB, and brace profiles are circular hollow sections (CHS).
2. Both chords and braces are of SHS.

The comparison is performed by employing topology optimization for given spans and truss heights. By using topology optimization, the best possible truss configurations for each combination of profiles is determined. This implies that the results are not biased by predetermined truss types that could be in favor of certain profile combination. In topology optimization, the combined manufacturing and material cost is minimized using a simplified cost function, with data provided by Ruukki.

Optimization is performed by assuming a pin-jointed structure, where bending is taken into account by a simplified heuristic approach. Moreover, joint strength checks are not included in optimization. As a post-processing step, the resulting trusses are evaluated by more accurate structural models and appropriate joint strength rules. The results of these evaluations are also reported.

2 Problem Setting

2.1 Overview

The trusses considered in are simply supported single-span roof trusses. The design domain is shown in Figure 2.1. The span of the truss is varied such that $L = 24\,\text{m}$, or $L = 36\,\text{m}$. For both spans, the height h can take the values $h = L/10$, and $h = L/20$. Thus, the geometry of the design domain implies 4 different cases.

For each variation of design domain geometry, two cross-section scenarios are considered:

1. Chords are HEA/HEB (S460), and the braces are CHS (S355);
2. Chords are SHS (S420), and the braces are SHS (S355).

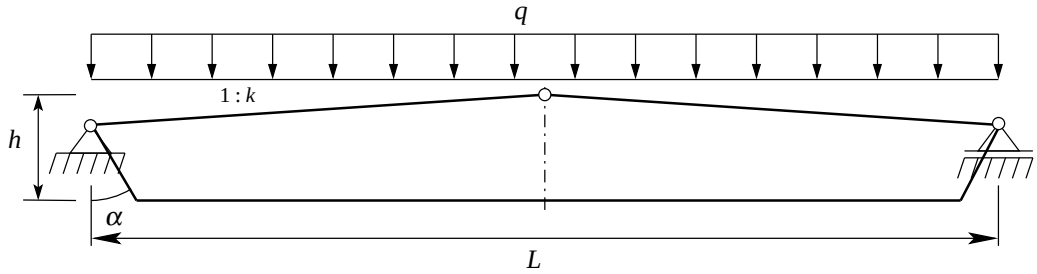

Figure 2.1: Design domain of the roof trusses.

The following loads are employed:

Dead load of roofing $0.5\,\text{kN/m}^2$

Self-weight of truss $0.16\,\text{kN/m}^2$

Snow $0.8 \cdot 2.5\,\text{kN/m}^2 = 2.0\,\text{kN/m}^2$

The distance between trusses is c/c = 6 m.

The design load is determined based on the Swedish National Annex of (EN 1990 2002):

$$\gamma_\text{d} \cdot 1.35 G_{kj,sup} \otimes \gamma_\text{d} \cdot 1.5 \psi_{0,1} Q_{k,1} \tag{2.1}$$

$$\gamma_\text{d} \cdot 0.89 \cdot 1.35 G_{kj,sup} \otimes \gamma_\text{d} \cdot 1.5 Q_{k,1} \tag{2.2}$$

With $\gamma_d = 1.0$, and $G_{kj,sup} = (0.5 + 0.16)\,\mathrm{kN/m^2} \cdot 6\,\mathrm{m} = 3.96\,\mathrm{kN/m}$, $Q_{k,1} = 2.0\,\mathrm{kN/m^2} \cdot 6\,\mathrm{m} = 12\,\mathrm{kN/m}$, and $\psi_{0,1} = 0.7$ for the snow load, the following is obtained:

$$q_1 = 1.0 \cdot 1.35 \cdot 3.96\,\mathrm{kN/m} + 1.0 \cdot 1.5 \cdot 0.7 \cdot 12\,\mathrm{kN/m} = 17.95\,\mathrm{kN/m} \quad (2.3)$$

$$q_2 = 1.0 \cdot 0.89 \cdot 1.35 \cdot 3.96\,\mathrm{kN/m} + 1.0 \cdot 1.5 \cdot 12\,\mathrm{kN/m} = 22.78\,\mathrm{kN/m} \quad (2.4)$$

Thus, the load employed is $q = \max\{q_1, q_2\} = 22.78\,\mathrm{kN/m}$.

2.2 Cross-section alternatives

2.2.1 HEA/HEB chords and CHS braces

The rules for welded joints between I-profile chords and hollow section braces state that the web height of the I-profiles must not exceed 400 mm (EN 1993–1–8 2005, Table 7.20). Furthermore, the cross-section must be in class 1 or 2 (with respect to compression). The largest applicable HEA profile is HEA 450, and the largest HEB profile is HEB 450. Consequently, there are 6 HEA and 16 HEB alternatives. The 22 available HEA/HEB profiles are given in Table 2.1.

Table 2.1: Available HEA/HEB cross-sections.

i	H [mm]	B [mm]	S [mm]	T [mm]	R [mm]	A [$10^2\,\mathrm{mm^2}$]	A_u [$10^3\,\mathrm{mm^2/mm}$]
1	96	100	5.0	8.0	12	21.20	0.56
2	114	120	5.0	8.0	12	25.30	0.68
3	133	140	5.5	8.5	12	31.40	0.79
4	152	160	6.0	9.0	15	38.80	0.91
5	350	300	10.0	17.5	27	142.80	1.83
6	390	300	11.0	19.0	27	159.00	1.91
7	100	100	6.0	10.0	12	26.00	0.57
8	120	120	6.5	11.0	12	34.00	0.69
9	140	140	7.0	12.0	12	43.00	0.81
10	160	160	8.0	13.0	15	54.30	0.92
11	180	180	8.5	14.0	15	65.30	1.04
12	200	200	9.0	15.0	18	78.10	1.15
13	220	220	9.5	16.0	18	91.00	1.27
14	240	240	10.0	17.0	21	106.00	1.38
15	260	260	10.0	17.5	24	118.40	1.50
16	280	280	10.5	18.0	24	131.40	1.62
17	300	300	11.0	19.0	27	149.10	1.73
18	320	300	11.5	20.5	27	161.30	1.77
19	340	300	12.0	21.5	27	470.90	1.81
20	360	300	12.5	22.5	27	180.60	1.85
21	400	300	13.5	24.0	27	197.80	1.93
22	450	300	14.0	26.0	27	218.00	2.03

For the CHS profiles, the following conditions are employed:

- Wall thickness must be at least 3 mm, which is according to Ruukki's recommendation ((EN 1993–1–8 2005, Clause 7.1.1(5)) requires a 2.5 mm wall thickness)
- Compression members must be in class 1.
- The ratio of the diameter, d_i, and the wall thickness, t_i, must satisfy

$$\frac{d_i}{t_i} \leq 50$$

  For S355, the limit of this ratio on cross-section class 3 is $90\varepsilon^2 = 90 \cdot (235/355) = 59.5775$. Thus, only some profiles of class 3 and none of the profiles of class 4 can be employed.
- The diameter of the profile must not exceed 300 mm. This is the maximum flange width of the available HEA/HEB profiles.

Requiring that the profiles belong to Ruukki's 'recommended series', 43 CHS alternatives are obtained. These are listed in Table 2.2. Of the 43 alternatives, only 3 belong to class 2, whereas the others are in class 1. For simplicity, these three alternatives (26, 35, 40) are removed from the profile set. Thus all CHS profiles belong to class 1.

2.2.2 Square hollow section chords and braces

The selection of square hollow sections (SHS) is chosen from the "recommended series" of Ruukki's profiles. The upper chord must be in class 1 (S420), whereas the lower chord must be in class 1 or 2 (S420). Compression braces must be in class 1 or 2, but for braces in tension, no limits for cross-section class are imposed. Nevertheless only class 1 and 2 profiles (S355) are chosen for all braces.

In addition to the restrictions to cross-section class, the following rules are employed in the cross-section selection:

1. Chord width is between 100 mm and 180 mm.
2. Minimum brace width is $0.35 \cdot 100\,\text{mm} = 35\,\text{mm}$. This requirement is derived from design rules for N-, K- and KT-joints. For other joint types, a similar but less stringent design rule is required, but here the more severe rule is used regardless of joint type.
3. Maximum brace width is $0.85 \cdot 180\,\text{mm} = 153\,\text{mm}$.
4. Wall thickness must be at least 3.0 mm.

With these rules, 44 profiles are included in the set of alternatives. They are listed in Table 2.3. For the braces, 40 profile alternatives are available. For the top and bottom chords, the number of profile alternatives are 22 and 24, respectively.

2.3 Cost Factors

In this study, the cost function includes the cost of material, blasting, and painting. The corresponding unit data is given in Table 2.4.

Table 2.2: Available CHS cross-sections.

i	D [mm]	T [mm]	A [10^2 mm^2]	A_u [10^3 mm^2/mm]
1	33.7	3.2	3.07	0.11
2	48.3	3.0	4.27	0.15
3	48.3	4.0	5.57	0.15
4	60.3	3.0	5.40	0.19
5	60.3	4.0	7.07	0.19
6	60.3	5.0	8.69	0.19
7	76.1	4.0	9.06	0.24
8	76.1	6.3	13.81	0.24
9	88.9	4.0	10.67	0.28
10	88.9	5.0	13.18	0.28
11	88.9	6.3	16.35	0.28
12	101.6	3.6	11.08	0.32
13	101.6	5.0	15.17	0.32
14	108.0	3.6	11.81	0.34
15	108.0	5.0	16.18	0.34
16	114.3	3.6	12.52	0.36
17	114.3	5.0	17.17	0.36
18	114.3	6.3	21.38	0.36
19	127.0	4.0	15.46	0.40
20	127.0	5.0	19.16	0.40
21	139.7	4.0	17.05	0.44
22	139.7	5.0	21.16	0.44
23	139.7	6.3	26.40	0.44
24	139.7	8.0	33.10	0.44
25	139.7	10.0	40.75	0.44
26	168.3	4.0	20.65	0.53
27	168.3	4.5	23.16	0.53
28	168.3	5.0	25.65	0.53
29	168.3	6.0	30.59	0.53
30	168.3	8.0	40.29	0.53
31	168.3	10.0	49.73	0.53
32	193.7	5.0	29.64	0.61
33	193.7	6.3	37.09	0.61
34	193.7	10.0	57.71	0.61
35	219.1	4.5	30.34	0.69
36	219.1	6.0	40.17	0.69
37	219.1	8.0	53.06	0.69
38	219.1	10.0	65.69	0.69
39	219.1	12.5	81.13	0.69
40	273.0	6.0	50.33	0.86
41	273.0	8.0	66.60	0.86
42	273.0	10.0	82.62	0.86
43	273.0	12.5	102.30	0.86

Table 2.3: Available SHS cross-sections. Profiles 1–40 are available for braces, profiles 21–44 can be chosen for the bottom chord, and profiles 21–44 except 28 and 36 can be selected for the top chord.

i	H [mm]	T [mm]	A [10^2 mm^2]	A_u [10^3 mm^2/mm]
1	40	3.0	4.21	0.15
2	40	4.0	5.35	0.15
3	50	3.0	5.41	0.19
4	50	4.0	6.95	0.19
5	50	5.0	8.36	0.18
6	60	3.0	6.61	0.23
7	60	4.0	8.55	0.23
8	60	5.0	10.36	0.22
9	70	3.0	7.81	0.27
10	70	4.0	10.15	0.27
11	70	5.0	12.36	0.26
12	80	3.0	9.01	0.31
13	80	4.0	11.75	0.31
14	80	5.0	14.36	0.30
15	80	6.0	16.83	0.30
16	90	3.0	10.21	0.35
17	90	4.0	13.35	0.35
18	90	5.0	16.36	0.34
19	90	6.0	19.23	0.34
20	100	3.0	11.41	0.39
21	100	4.0	14.95	0.39
22	100	5.0	18.36	0.38
23	100	6.0	21.63	0.38
24	100	8.0	27.24	0.37
25	110	4.0	16.55	0.43
26	110	5.0	20.36	0.42
27	110	6.0	24.03	0.42
28	120	4.0	18.15	0.47
29	120	5.0	22.36	0.46
30	120	6.0	26.43	0.46
31	120	8.0	33.64	0.45
32	120	10.0	40.57	0.44
33	140	5.0	26.36	0.54
34	140	6.0	31.23	0.54
35	140	8.0	40.04	0.53
36	150	5.0	28.36	0.58
37	150	6.0	33.63	0.58
38	150	8.0	43.24	0.57
39	150	10.0	52.57	0.56
40	150	12.5	62.04	0.54
41	160	8.0	46.44	0.61
42	160	10.0	56.57	0.60
43	180	8.0	52.84	0.69
44	180	10.0	64.57	0.68

Table 2.4: Cost data.

Factor	Cost	Unit
Blasting	3	€/m^2
Painting, C2	8.5	€/m^2
Intumescent Paint, R30	40	€/m^2
Quality control	20	€/(10^3 kg)
HEA & HEB, S355	750	€/(10^3 kg)
HEA & HEB, S460	800	€/(10^3 kg)
CHS, S355	750	€/(10^3 kg)
SHS, S420/S355	750	€/(10^3 kg)

Material cost. The cost of material is expressed as

$$C_M(\mathbf{x}) = \sum_{i=1}^{n_E} \sum_j c_{M,j} \rho_i L_i \hat{A}_j y_{ij} \tag{2.5}$$

where $c_{M,i}$ is the material cost factor that is specific for profile j.

Blasting cost. The cost of blasting is written as

$$C_B(\mathbf{x}) = \sum_{i=1}^{n_E} \sum_j c_B L_i \hat{A}_{u,j} y_{ij} \tag{2.6}$$

where $c_B = 3 \cdot 10^{-6} €/\text{mm}^2$ is the blasting cost factor.

Painting cost. In general, the cost of painting can be expressed as

$$C_P(\mathbf{x}) = \sum_{i=1}^{n_E} \sum_j c_P L_i \hat{A}_{u,j} y_{ij} \tag{2.7}$$

where $c_B = 8.5 \cdot 10^{-6} €/\text{mm}^2$ is the unit cost for painting.
The complete cost function is the sum of the above cost factors, i.e

$$C(\mathbf{x}) = C_M(\mathbf{x}) + C_B(\mathbf{x}) + C_P(\mathbf{x}) \tag{2.8}$$

3 Topology Optimization

3.1 Introduction

As a first step in the study, optimum topologies for varying truss spans and heights are determined. In topology optimization, the structural model is based on pin-jointed truss elements, where only axial forces appear. In the basic model, the effects of bending are neglected. However, for the specific application, the chord members are sized for bending by approximating the bending moment and applying the appropriate design rule of Eurocode 3. The framework for topology optimization can be summarized as follows.

- Members are pin-jointed bars.
- Bending of the chords is taken into account by assuming a bending moment of

  $$M_i = \frac{qL_i^2}{10}$$

  in the top chord members and

  $$M_i = \frac{qL_i^2}{20}$$

  in the bottom chord members. In the above, q is the design load, and L_i is the length of member i. Members in tension must satisfy the appropriate design rule in (EN 1993–1–1 2005, Clause 6.2.9.1(5)), and members in tension are sized according to the rule (EN 1993–1–1 2005, Clause 6.3.3(4)).
- Joints are not considered, i.e. joint strength and eccentricities are not checked. However, separate constraints ensure that the dimensions of the braces are within the prescribed limits as stated in (EN 1993–1–8 2005, Table 7.20 and Table 7.8). To be more specific, for the SHS profiles, the rules of first column of (EN 1993–1–8 2005, Table 7.8) are implemented. Furthermore, it is ensured that the brace widths do not exceed the width of the chords.
- The trusses are optimized for cost.
- The height of the truss is measured from the center line of the bottom chord to the center line of the top chord at the ridge.

For each combination of span and height, 3 ground structures are considered. One half of the design domain is divided into 8, 10, or 12 equally spaced intervals. Braces are added to the ground structure, if they meet both chords in an angle greater than 30°. The maximum member length is limited to $L/5$. The ground structures are depicted in Figure 3.1.

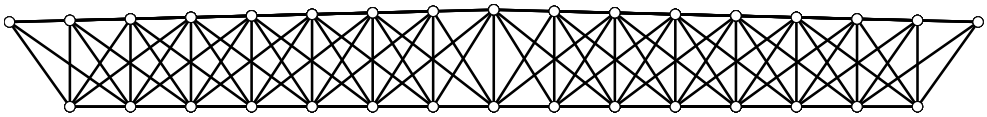

(a) Ground structure with 8 intervals on one half of the span, $h = L/10$.

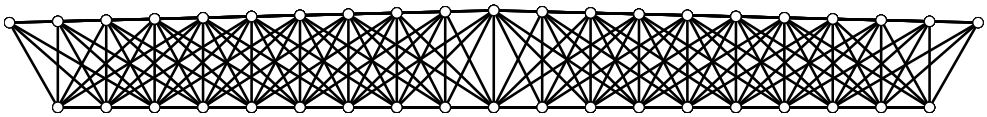

(b) Ground structure with 10 intervals on one half of the span, $h = L/10$.

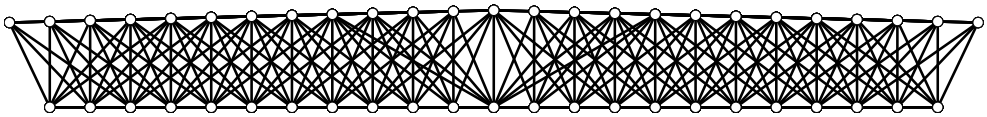

(c) Ground structure with 12 intervals on one half of the span, $h = L/10$.

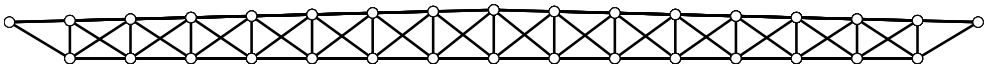

(d) Ground structure with 8 intervals on one half of the span, $h = L/20$.

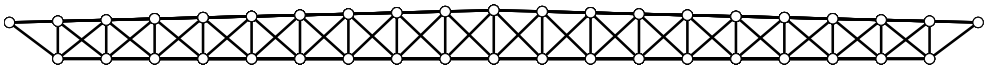

(e) Ground structure with 10 intervals on one half of the span, $h = L/20$.

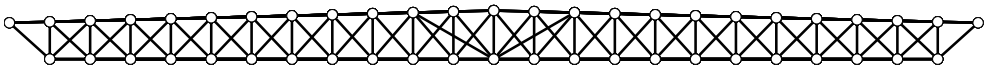

(f) Ground structure with 12 intervals on one half of the span, $h = L/20$.

Figure 3.1: Ground structures for topology optimization, $L = 24\,\text{m}$.

3.2 HEA/HEB chords and CHS braces

For HEA/HEB profiles, there are 22 available alternatives that belong to cross-section class 1 or 2 (S460) and have diameter at most 400 mm. For CHS braces belonging to class 1 (S355), 40 alternatives are available. The number of profile alternatives has a direct effect on the optimization problem size. In Table 3.1, the different problem instances are shown.

The results of topology optimization are summarized in Table 3.2. In the table, the initial and minimum cost are reported. For given span and height, the minimum cost among the three ground structures is in bold face. It can be seen that depending on the span and height, any ground structure can provide the minimum cost.

The optimum designs are illustrated in Figures 3.2–3.5, and member details are shown in Tables 3.3–3.6. For each member, the profile, cost, axial force, design value of bending moment, and utilization ratios for strength and buckling design rules are given. Note that due to symmetry, only half of the members are displayed in the tables. Note that the utilization ratios are given with respect to normal force resistances, also for chord members.

Table 3.1: Problem instances for topology optimization of HEA/HEB/CHS trusses.

i	q [kN/m]	L [m]	L/h	k	n_x	N_x	N_y	$n^{\leq}$	$n^{=}$	n_E
1	22.78	24	10	40	8	7268	2457	21617	275	150
2	22.78	24	10	40	10	11651	3923	35042	394	237
3	22.78	24	10	40	12	15103	5071	45958	502	313
4	22.78	24	20	40	8	5669	1924	17139	249	124
5	22.78	24	20	40	10	7715	2611	23676	330	173
6	22.78	24	20	40	12	10183	3431	31688	422	233
7	22.78	36	10	40	8	7268	2457	21617	275	150
8	22.78	36	10	40	10	11651	3923	35042	394	237
9	22.78	36	10	40	12	15103	5071	45958	502	313
10	22.78	36	20	40	8	5669	1924	17139	249	124
11	22.78	36	20	40	10	7715	2611	23676	330	173
12	22.78	36	20	40	12	10183	3431	31688	422	233

Table 3.2: Results of topology optimization for HEA/HEB/CHS trusses. C_0 = initial cost; C^* = minimum cost obtained; t^* = runtime when the optimum was found; t_{fin} = runtime at termination (time limit 21600 s); G_0 = initial optimality gap; G^* = optimality gap, when optimum was found; G_{fin} = final optimality gap.

i	C_0 [10^2 €]	C^* [10^2 €]	$\frac{C_0 - C^*}{C^*}$ [%]	t^* [s]	t_{fin}	G_0 [%]	G^* [%]	G_{fin} [%]
1	13.60	**13.37**	1.69	32	248	28.90	13.40	1.98
2	14.73	14.32	2.86	429	666	33.00	12.30	1.67
3	15.24	14.01	8.79	1476	3180	37.10	15.40	1.44
4	17.10	17.07	0.16	194	257	26.20	11.70	1.81
5	17.28	17.14	0.79	465	731	29.20	13.80	1.05
6	16.53	**16.36**	1.01	1078	3109	25.90	12.00	2.00
7	29.89	**29.73**	0.55	564	603	33.10	7.04	1.88
8	36.13	35.10	2.94	238	890	45.20	30.10	1.84
9	34.14	32.56	4.86	7922	7944	42.70	2.22	1.61
10	38.93	38.75	0.46	247	249	29.90	4.35	1.20
11	36.14	**35.99**	0.44	785	1367	27.70	13.50	1.39
12	36.40	36.22	0.50	692	1340	29.00	18.60	1.04

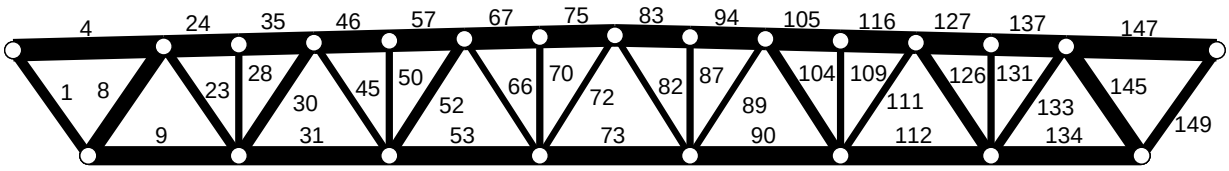

Figure 3.2: Optimum topology for HEA/HEB/CHS profiles. $L = 24\,\text{m}$, $h = L/10$. $C^* = 1337$€.

Table 3.3: Optimum design for $L = 24\,\text{m}$, $h = L/10$. The axial forces and design values of the bending moment are given. Furthermore, the utilization ratio for strength, U_S, and stability, U_B, are reported. Due to symmetry, only the members on the left to the symmetry axis are shown.

i	Profile	C [€]	N [kN]	M_{Ed} [kNm]	U_S	U_B
1	CHS 60.3x5.0	38.33	288.78	0.00	0.94	0.00
4	HEB 100	139.58	-167.91	20.51	0.23	0.97
8	CHS 88.9x6.3	69.18	-285.46	0.00	0.49	0.97
9	HEA 100	120.59	329.92	20.50	0.44	0.00
23	CHS 60.3x4.0	34.07	214.58	0.00	0.85	0.00
24	HEB 100	69.79	-451.88	5.13	0.42	0.56
28	CHS 48.3x3.0	19.16	-34.17	0.00	0.23	0.81
30	CHS 88.9x4.0	52.23	-171.23	0.00	0.45	0.89
31	HEA 100	120.59	546.72	20.50	0.73	0.00
35	HEB 100	69.79	-451.88	5.13	0.42	0.56
45	CHS 48.3x3.0	23.41	125.22	0.00	0.83	0.00
46	HEB 100	69.79	-616.37	5.13	0.57	0.77
50	CHS 48.3x3.0	19.81	-34.17	0.00	0.23	0.86
52	CHS 76.1x4.0	45.51	-83.33	0.00	0.26	0.65
53	HEA 100	120.59	661.35	20.50	0.89	0.00
57	HEB 100	69.79	-616.37	5.13	0.57	0.77
66	CHS 33.7x3.2	17.01	40.66	0.00	0.37	0.00
67	HEB 100	69.79	-683.61	5.13	0.63	0.85
70	CHS 48.3x3.0	20.45	-34.17	0.00	0.23	0.90
72	CHS 33.7x3.2	17.40	-0.00	0.00	0.00	0.00
73	HEA 100	60.29	683.40	20.50	0.92	0.00
75	HEB 100	69.79	-683.61	5.13	0.63	0.85
Total Cost		1336.96				

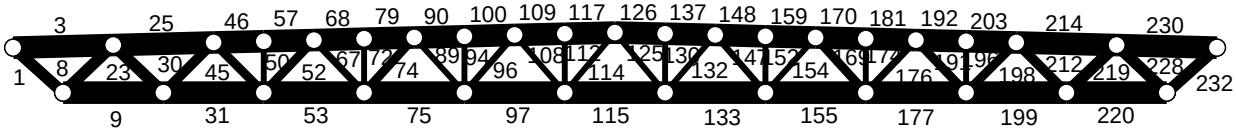

Figure 3.3: Optimum topology for HEA/HEB/CHS profiles. $L = 24\,\text{m}$, $h = L/20$. $C^* = 1636$€.

Table 3.4: Optimum design for $L = 24\,\text{m}$, $h = L/20$. The axial forces and design values of the bending moment are given. Furthermore, the utilization ratio for strength, U_S, and stability, U_B, are reported. Due to symmetry, only the members on the left to the symmetry axis are shown.

i	Profile	C [€]	N [kN]	M_{Ed} [kNm]	U_S	U_B
1	CHS 76.1x6.3	29.86	364.46	0.00	0.74	0.00
3	HEB 120	119.14	-270.98	9.12	0.19	0.28
8	CHS 76.1x6.3	30.61	-353.99	0.00	0.72	0.96
9	HEB 120	119.10	527.54	9.11	0.36	0.00
23	CHS 76.1x6.3	30.61	271.38	0.00	0.55	0.00
25	HEB 120	119.14	-724.51	9.12	0.52	0.76
30	CHS 88.9x4.0	27.32	-264.33	0.00	0.70	0.86
31	HEB 120	119.10	911.20	9.11	0.62	0.00
45	CHS 60.3x5.0	21.00	204.30	0.00	0.66	0.00
46	HEB 120	59.57	-1055.99	2.28	0.69	0.74
50	CHS 33.7x3.2	6.30	-22.78	0.00	0.21	0.44
52	CHS 60.3x5.0	21.54	-168.03	0.00	0.54	0.88
53	HEB 120	119.10	1171.54	9.11	0.79	0.00
57	HEB 120	59.57	-1055.99	2.28	0.69	0.74
67	CHS 48.3x4.0	14.83	129.49	0.00	0.65	0.00
68	HEB 120	59.57	-1261.24	2.28	0.83	0.89
72	CHS 33.7x3.2	6.61	-22.78	0.00	0.21	0.47
74	CHS 60.3x5.0	22.08	-95.94	0.00	0.31	0.51
75	HEB 120	119.10	1325.38	9.11	0.90	0.00
79	HEB 120	59.57	-1261.24	2.28	0.83	0.89
89	CHS 33.7x3.2	9.14	61.57	0.00	0.56	0.00
90	HEB 120	59.57	-1367.23	2.28	0.90	0.96
94	CHS 33.7x3.2	6.92	-22.78	0.00	0.21	0.49
96	CHS 48.3x3.0	13.19	-30.19	0.00	0.20	0.42
97	HEB 120	119.10	1386.61	9.11	0.94	0.00
100	HEB 120	59.57	-1367.23	2.28	0.90	0.96
108	CHS 33.7x3.2	9.37	-0.64	0.00	0.01	0.02
109	HEB 120	59.57	-1386.62	2.28	0.91	0.98
112	CHS 33.7x3.2	7.23	-22.78	0.00	0.21	0.52
114	CHS 33.7x3.2	9.61	30.28	0.00	0.28	0.00
115	HEB 120	59.55	1366.80	9.11	0.92	0.00
117	HEB 120	59.57	-1386.62	2.28	0.91	0.98
Total Cost		1636.08				

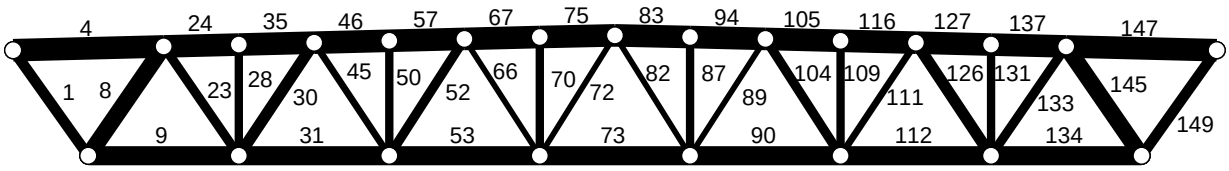

Figure 3.4: Optimum topology for HEA/HEB/CHS profiles. $L = 36\,\text{m}$, $h = L/10$. $C^* = 2973$€.

Table 3.5: Optimum design for $L = 36\,\text{m}$, $h = L/10$. The axial forces and design values of the bending moment are given. Furthermore, the utilization ratio for strength, U_S, and stability, U_B, are reported. Due to symmetry, only the members on the left to the symmetry axis are shown.

i	Profile	C [€]	N [kN]	M_{Ed} [kNm]	U_S	U_B
1	CHS 76.1x6.3	85.91	433.18	0.00	0.88	0.00
4	HEA 160	318.65	-251.86	46.16	0.22	0.87
8	CHS 139.7x6.3	166.50	-428.19	0.00	0.46	0.84
9	HEA 140	264.09	494.88	46.13	0.46	0.00
23	CHS 88.9x4.0	76.55	321.86	0.00	0.85	0.00
24	HEA 160	159.33	-677.82	11.54	0.42	0.55
28	CHS 60.3x5.0	49.29	-51.25	0.00	0.17	0.84
30	CHS 127.0x4.0	113.03	-256.84	0.00	0.47	0.96
31	HEA 140	264.09	820.08	46.13	0.76	0.00
35	HEA 160	159.33	-677.82	11.54	0.42	0.55
45	CHS 48.3x4.0	41.49	187.83	0.00	0.95	0.00
46	HEA 160	159.33	-924.56	11.54	0.57	0.74
50	CHS 60.3x5.0	50.96	-51.25	0.00	0.17	0.89
52	CHS 101.6x3.6	86.04	-124.99	0.00	0.32	0.92
53	HEA 140	264.09	992.03	46.13	0.92	0.00
57	HEA 160	159.33	-924.56	11.54	0.57	0.74
66	CHS 33.7x3.2	25.52	61.00	0.00	0.56	0.00
67	HEA 160	159.33	-1025.42	11.54	0.63	0.83
70	CHS 60.3x5.0	52.63	-51.26	0.00	0.17	0.94
72	CHS 33.7x3.2	26.11	0.00	0.00	0.00	0.00
73	HEA 140	132.04	1025.10	46.13	0.95	0.00
75	HEA 160	159.33	-1025.42	11.54	0.63	0.83
Total Cost		2972.95				

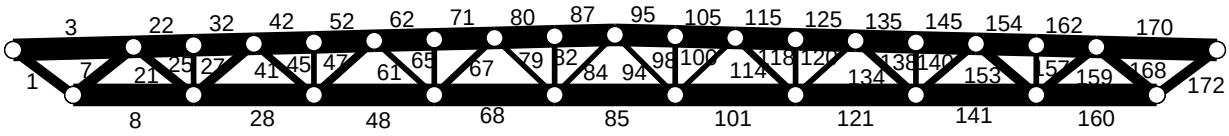

Figure 3.5: Optimum topology for HEA/HEB/CHS profiles. $L = 36\,\text{m}$, $h = L/20$. $C^* = 3599\,€$.

Table 3.6: Optimum design for $L = 36\,\text{m}$, $h = L/20$. The axial forces and design values of the bending moment are given. Furthermore, the utilization ratio for strength, U_S, and stability, U_B, are reported. Due to symmetry, only the members on the left to the symmetry axis are shown.

i	Profile	C [€]	N [kN]	M_{Ed} [kNm]	U_S	U_B
1	CHS 114.3x5.0	65.28	595.22	0.00	0.98	0.00
3	HEB 160	327.77	-476.32	29.54	0.23	0.50
7	CHS 139.7x5.0	82.24	-571.69	0.00	0.76	0.95
8	HEB 160	327.67	922.59	29.52	0.40	0.00
21	CHS 76.1x6.3	51.16	441.57	0.00	0.90	0.00
22	HEB 160	163.89	-1267.79	7.39	0.53	0.61
25	CHS 48.3x3.0	12.86	-41.00	0.00	0.27	0.55
27	CHS 108.0x5.0	64.63	-362.61	0.00	0.63	0.92
28	HEB 160	327.67	1543.68	29.52	0.67	0.00
32	HEB 160	163.89	-1267.79	7.39	0.53	0.61
41	CHS 60.3x5.0	35.09	280.38	0.00	0.91	0.00
42	HEB 160	163.89	-1757.86	7.39	0.73	0.84
45	CHS 48.3x3.0	13.64	-41.00	0.00	0.27	0.59
47	CHS 88.9x4.0	46.78	-210.15	0.00	0.55	0.97
48	HEB 160	327.67	1913.52	29.52	0.83	0.00
52	HEB 160	163.89	-1757.86	7.39	0.73	0.84
61	CHS 48.3x3.0	20.97	139.16	0.00	0.92	0.00
62	HEB 160	163.89	-2017.58	7.39	0.84	0.97
65	CHS 48.3x3.0	14.42	-41.00	0.00	0.27	0.64
67	CHS 60.3x4.0	32.01	-75.62	0.00	0.30	0.92
68	HEB 160	327.67	2071.78	29.52	0.90	0.00
71	HEB 160	163.89	-2017.58	7.39	0.84	0.97
79	CHS 33.7x3.2	15.27	13.74	0.00	0.13	0.00
80	HEB 160	163.89	-2082.39	7.39	0.87	1.00
82	CHS 48.3x3.0	15.19	-41.00	0.00	0.27	0.69
84	CHS 33.7x3.2	15.65	44.61	0.00	0.41	0.00
85	HEB 160	163.84	2050.20	29.52	0.89	0.00
87	HEB 160	163.89	-2082.39	7.39	0.87	1.00
Total Cost		3598.56				

3.3 SHS chord and SHS braces

For SHS trusses, same ground structures are used as for the HEA/HEB/CHS trusses (see Figure 3.1). Problem sizes for each instance are given in Table 3.7.

Two sets of optimization problems are solved regarding the buckling curve. In the first run, the buckling curve 'c' required by the present Eurocode is employed. Then, due to the implied results of recent measurements, buckling curve 'b' is adopted for the members. The results for these separate instances are reported below.

Table 3.7: Problem instances for topology optimization of SHS trusses.

i	q [kN/m]	L [m]	L/h	k	n_x	N_x	N_y	$n^{\leq}$	$n^{=}$	n_E
1	22.78	24	10	40	8	7384	2497	22131	275	150
2	22.78	24	10	40	10	11843	3989	35906	394	237
3	22.78	24	10	40	12	15343	5153	47042	502	313
4	22.78	24	20	40	8	5785	1964	17601	249	124
5	22.78	24	20	40	10	7907	2677	24412	330	173
6	22.78	24	20	40	12	10423	3513	32612	422	233
7	22.78	36	10	40	8	7384	2497	22131	275	150
8	22.78	36	10	40	10	11843	3989	35906	394	237
9	22.78	36	10	40	12	15343	5153	47042	502	313
10	22.78	36	20	40	8	5785	1964	17601	249	124
11	22.78	36	20	40	10	7907	2677	24412	330	173
12	22.78	36	20	40	12	10423	3513	32612	422	233

3.3.1 Results using present Eurocode

First, the SHS trusses are optimized using present Eurocode. This means that the buckling curve 'c' as indicated in (EN 1993–1–1 2005, Table 6.2) is employed for cold-formed sections. The results of topology optimization are summarized in Table 3.8. It can be seen that the algorithm converged within one hour in all cases, and usually in much less time.

From the results, it can be seen that for both spans the trusses with height $h = L/10$ are substantially more economical. For the 24 m span, the difference is 28 %, and for the span of 36 m, the difference is 20 %.

The optimum topologies are shown in Figures 3.6–3.9, and the corresponding member data are given in Tables 3.9–3.12. In addition to member profiles, the normal forces, bending moments, and utilization ratios are also given.

Table 3.8: Results of topology optimization for SHS trusses. C_0 = initial cost; C^* = minimum cost obtained; t^* = runtime when the optimum was found; t_{fin} = runtime at termination (time limit 21600 s); G_0 = initial optimality gap; G^* = optimality gap, when optimum was found; G_{fin} = final optimality gap.

i	C_0 [10^2 €]	C^* [10^2 €]	$\frac{C_0 - C^*}{C^*}$ [%]	t^* [s]	t_{fin}	G_0 [%]	G^* [%]	G_{fin} [%]
1	12.72	**12.18**	4.47	424	430	28.50	2.33	1.93
2	13.74	13.11	4.81	675	763	32.50	8.59	1.06
3	13.49	12.54	7.58	2963	3311	33.60	6.72	1.93
4	16.39	16.29	0.63	29	278	25.90	16.30	1.95
5	16.48	**15.61**	5.55	644	1103	28.10	9.70	1.94
6	16.88	15.79	6.89	1528	3463	30.30	11.70	2.00
7	28.75	**28.03**	2.59	298	455	31.90	15.20	1.97
8	31.40	30.03	4.57	571	627	34.80	10.50	1.79
9	30.43	28.75	5.87	2081	2484	36.00	7.43	2.00
10	37.06	35.50	4.40	41	50	21.60	6.29	0.59
11	35.28	34.53	2.18	541	541	22.90	1.77	1.67
12	35.32	**33.75**	4.64	1932	1932	26.20	2.15	1.88

3.3.2 Results using buckling curve b

The results of optimization using the buckling curve 'b' of (EN 1993–1–1 2005) are summarized in Table 3.13. When the minimum costs obtained are compared with the minimum costs of the previous Section (see Table 3.8), it can be seen that for the trusses with $h = L/10$, the cost saving is 1.5 % and 2.0 % for the spans 24 m and 36 m, respectively. For the lower trusses (with $h = L/20$), the cost savings for both spans are only 0.3 %.

As in the previous Section, the higher trusses ($h = L/10$) are significantly more economical (30 %, and 22 %).

The optimum topologies are depicted in Figures 3.10–3.13, and the corresponding member data are given in Tables 3.14–3.17.

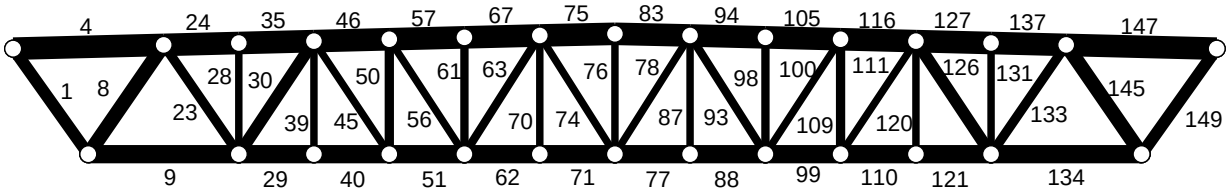

Figure 3.6: Optimum topology for SHS profiles. $L = 24\,\text{m}$, $h = L/10$. $C^* = 1218$€.

Table 3.9: Optimum SHS truss design for $L = 24\,\text{m}$, $h = L/10$. The axial forces and design values of the bending moment are given. Furthermore, the utilization ratio for strength, U_S, and stability, U_B, are reported. Due to symmetry, only the members on the left to the symmetry axis are shown.

i	Profile	C [€]	N [kN]	M_{Ed} [kNm]	U_S	U_B
1	SHS 90x3.0	52.63	288.78	0.00	0.80	0.00
4	SHS 110x6.0	116.10	-167.91	20.51	0.28	0.82
8	SHS 90x4.0	63.67	-285.46	0.00	0.60	1.00
9	SHS 100x5.0	93.01	329.92	10.25	0.60	0.00
23	SHS 50x4.0	33.50	214.58	0.00	0.87	0.00
24	SHS 110x6.0	58.05	-451.88	5.13	0.50	0.62
28	SHS 40x3.0	18.89	-34.17	0.00	0.23	0.93
29	SHS 100x5.0	46.51	546.72	2.56	0.76	0.00
30	SHS 90x3.0	55.15	-171.23	0.00	0.47	0.79
35	SHS 110x6.0	58.05	-451.88	5.13	0.50	0.62
39	SHS 40x3.0	19.21	-0.00	0.00	0.00	0.00
40	SHS 100x5.0	46.51	546.72	2.56	0.76	0.00
45	SHS 40x3.0	23.09	125.22	0.00	0.84	0.00
46	SHS 110x6.0	58.05	-616.37	5.13	0.68	0.84
50	SHS 60x3.0	30.38	-104.19	0.00	0.44	0.99
51	SHS 100x5.0	46.51	616.18	2.56	0.86	0.00
56	SHS 40x3.0	23.36	82.38	0.00	0.55	0.00
57	SHS 110x6.0	58.05	-661.56	5.13	0.73	0.90
61	SHS 40x4.0	22.84	-34.17	0.00	0.18	0.84
62	SHS 100x5.0	46.51	683.40	2.56	0.96	0.00
63	SHS 50x3.0	30.53	-41.13	0.00	0.21	0.86
67	SHS 110x6.0	58.05	-661.56	5.13	0.73	0.90
70	SHS 40x3.0	20.17	0.00	0.00	0.00	0.00
71	SHS 100x5.0	46.51	683.40	2.56	0.96	0.00
74	SHS 40x3.0	23.90	0.00	0.00	0.00	0.00
75	SHS 110x6.0	58.05	-683.61	5.13	0.75	0.93
76	SHS 40x3.0	10.25	-0.00	0.00	0.00	0.00
Total Cost		1217.51				

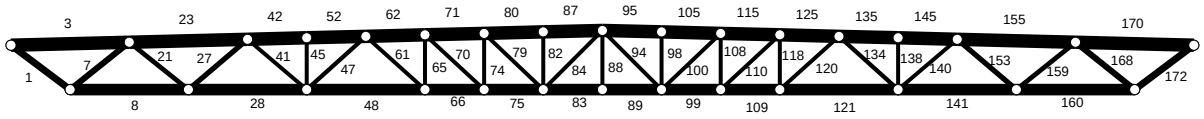

Figure 3.7: Optimum topology for SHS profiles. $L = 24\,\text{m}$, $h = L/20$. $C^* = 1561$€.

Table 3.10: Optimum design for $L = 24\,\text{m}$, $h = L/20$. The axial forces and design values of the bending moment are given. Furthermore, the utilization ratio for strength, U_S, and stability, U_B, are reported. Due to symmetry, only the members on the left to the symmetry axis are shown.

i	Profile	C [€]	N [kN]	M_{Ed} [kNm]	U_S	U_B
1	SHS 110x4.0	44.71	396.81	0.00	0.68	0.00
3	SHS 120x10.0	141.87	-317.55	13.13	0.22	0.35
7	SHS 90x4.0	37.03	-381.13	0.00	0.80	0.97
8	SHS 120x8.0	122.22	615.06	6.56	0.48	0.00
21	SHS 50x5.0	22.00	273.16	0.00	0.92	0.00
23	SHS 120x10.0	141.87	-828.62	13.13	0.57	0.91
27	SHS 90x3.0	32.12	-263.48	0.00	0.73	0.88
28	SHS 120x8.0	122.22	1029.12	6.56	0.80	0.00
41	SHS 50x3.0	17.18	186.92	0.00	0.97	0.00
42	SHS 120x10.0	70.94	-1171.91	3.28	0.72	0.79
45	SHS 50x3.0	11.46	-27.34	0.00	0.14	0.19
47	SHS 60x3.0	21.44	-140.10	0.00	0.60	0.92
48	SHS 120x8.0	122.22	1275.68	6.56	0.99	0.00
52	SHS 120x10.0	70.94	-1171.91	3.28	0.72	0.79
61	SHS 50x3.0	17.61	92.77	0.00	0.48	0.00
62	SHS 120x10.0	70.94	-1345.06	3.28	0.82	0.91
65	SHS 50x3.0	12.11	-62.06	0.00	0.32	0.44
66	SHS 120x8.0	61.11	1344.64	1.64	0.97	0.00
70	SHS 50x3.0	17.83	49.79	0.00	0.26	0.00
71	SHS 120x10.0	70.94	-1381.62	3.28	0.84	0.93
74	SHS 50x3.0	12.44	-33.81	0.00	0.18	0.24
75	SHS 120x8.0	61.11	1381.19	1.64	1.00	0.00
79	SHS 50x3.0	18.06	9.16	0.00	0.05	0.00
80	SHS 120x10.0	70.94	-1388.26	3.28	0.85	0.93
82	SHS 50x3.0	12.76	-27.34	0.00	0.14	0.20
83	SHS 120x8.0	61.11	1366.80	1.64	0.99	0.00
84	SHS 50x3.0	18.52	29.74	0.00	0.15	0.00
87	SHS 120x10.0	70.94	-1388.26	3.28	0.85	0.93
88	SHS 50x3.0	6.55	0.00	0.00	0.00	0.00
Total Cost		1561.18				

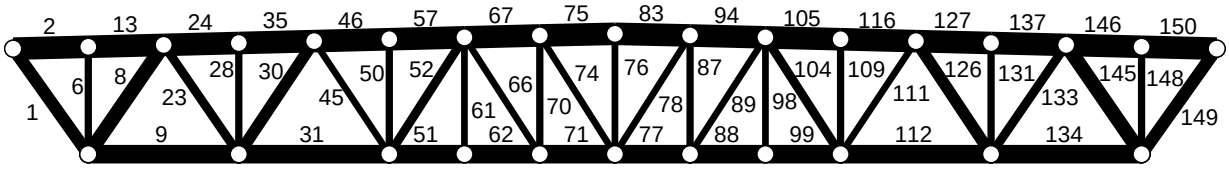

Figure 3.8: Optimum topology for SHS profiles. $L = 36\,\text{m}$, $h = L/10$. $C^* = 2803\,€$.

Table 3.11: Optimum design for $L = 36\,\text{m}$, $h = L/10$. The axial forces and design values of the bending moment are given. Furthermore, the utilization ratio for strength, U_S, and stability, U_B, are reported. Due to symmetry, only the members on the left to the symmetry axis are shown.

i	Profile	C [€]	N [kN]	M_{Ed} [kNm]	U_S	U_B
1	SHS 120x4.0	126.43	464.12	0.00	0.72	0.00
2	SHS 140x8.0	136.17	-269.85	11.54	0.18	0.24
6	SHS 60x3.0	42.58	-51.25	0.00	0.22	0.80
8	SHS 120x5.0	149.33	-396.51	0.00	0.50	0.93
9	SHS 140x6.0	225.68	494.88	23.06	0.52	0.00
13	SHS 140x8.0	136.17	-269.85	11.54	0.18	0.24
23	SHS 60x5.0	69.96	321.86	0.00	0.88	0.00
24	SHS 140x8.0	136.17	-677.82	11.54	0.45	0.60
28	SHS 60x3.0	44.08	-51.25	0.00	0.22	0.84
30	SHS 110x4.0	120.90	-256.84	0.00	0.44	0.91
31	SHS 140x6.0	225.68	820.08	23.06	0.86	0.00
35	SHS 140x8.0	136.17	-677.82	11.54	0.45	0.60
45	SHS 50x3.0	44.25	187.83	0.00	0.98	0.00
46	SHS 140x8.0	136.17	-924.56	11.54	0.62	0.82
50	SHS 60x3.0	45.57	-51.25	0.00	0.22	0.89
51	SHS 140x6.0	112.84	992.03	5.77	0.81	0.00
52	SHS 90x3.0	84.64	-124.99	0.00	0.34	0.97
57	SHS 140x8.0	136.17	-924.56	11.54	0.62	0.82
61	SHS 50x3.0	38.05	0.00	0.00	0.00	0.00
62	SHS 140x6.0	112.84	992.03	5.77	0.81	0.00
66	SHS 50x3.0	45.28	61.00	0.00	0.32	0.00
67	SHS 140x8.0	136.17	-1025.42	11.54	0.69	0.91
70	SHS 60x3.0	47.06	-51.25	0.00	0.22	0.94
71	SHS 140x6.0	112.84	1025.10	5.77	0.84	0.00
74	SHS 50x3.0	45.80	-0.00	0.00	0.00	0.00
75	SHS 140x8.0	136.17	-1025.42	11.54	0.69	0.91
76	SHS 50x3.0	19.64	-0.00	0.00	0.00	0.00
Total Cost		2802.82				

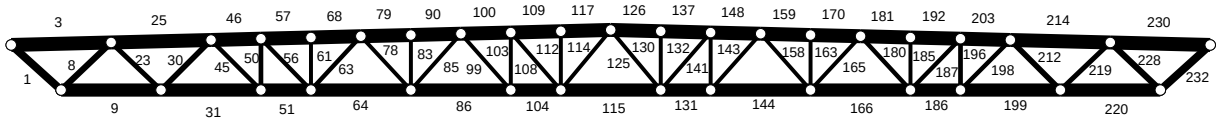

Figure 3.9: Optimum topology for SHS profiles. $L = 36\,\text{m}$, $h = L/20$. $C^* = 3375\,€$.

Table 3.12: Optimum design for $L = 36\,\text{m}$, $h = L/20$. The axial forces and design values of the bending moment are given. Furthermore, the utilization ratio for strength, U_S, and stability, U_B, are reported. Due to symmetry, only the members on the left to the symmetry axis are shown.

i	Profile	C [€]	N [kN]	M_{Ed} [kNm]	U_S	U_B
1	SHS 140x5.0	89.51	546.68	0.00	0.58	0.00
3	SHS 160x10.0	246.43	-406.47	20.51	0.20	0.28
8	SHS 120x4.0	67.57	-530.98	0.00	0.82	0.99
9	SHS 150x10.0	229.09	791.31	10.25	0.39	0.00
23	SHS 80x4.0	43.95	407.07	0.00	0.98	0.00
25	SHS 160x10.0	246.43	-1086.77	20.51	0.52	0.76
30	SHS 100x4.0	57.17	-396.50	0.00	0.75	0.98
31	SHS 150x10.0	229.09	1366.80	10.25	0.67	0.00
45	SHS 80x3.0	38.23	306.44	0.00	0.96	0.00
46	SHS 160x10.0	123.22	-1583.98	5.13	0.69	0.74
50	SHS 60x5.0	27.14	-216.69	0.00	0.59	0.91
51	SHS 150x10.0	114.54	1583.49	2.56	0.73	0.00
56	SHS 60x4.0	33.37	248.92	0.00	0.82	0.00
57	SHS 160x10.0	123.22	-1757.86	5.13	0.76	0.82
61	SHS 60x3.0	20.92	-34.17	0.00	0.15	0.22
63	SHS 80x3.0	39.69	-196.67	0.00	0.61	0.96
64	SHS 150x10.0	229.09	1891.27	10.25	0.92	0.00
68	SHS 160x10.0	123.22	-1757.86	5.13	0.76	0.82
78	SHS 60x3.0	29.25	142.13	0.00	0.61	0.00
79	SHS 160x10.0	123.22	-1988.69	5.13	0.86	0.93
83	SHS 60x3.0	21.91	-34.17	0.00	0.15	0.23
85	SHS 60x3.0	29.99	-93.51	0.00	0.40	0.87
86	SHS 150x10.0	229.09	2050.20	10.25	1.00	0.00
90	SHS 160x10.0	123.22	-1988.69	5.13	0.86	0.93
99	SHS 60x3.0	29.99	44.72	0.00	0.19	0.00
100	SHS 160x10.0	123.22	-2080.56	5.13	0.90	0.98
103	SHS 60x3.0	22.91	-33.43	0.00	0.14	0.23
104	SHS 150x10.0	114.54	2079.91	2.56	0.96	0.00
108	SHS 60x3.0	30.36	-0.96	0.00	0.00	0.01
109	SHS 160x10.0	123.22	-2079.93	5.13	0.90	0.97
112	SHS 60x3.0	23.41	-34.17	0.00	0.15	0.24
114	SHS 60x3.0	31.12	45.43	0.00	0.19	0.00
115	SHS 150x10.0	114.54	2050.20	10.25	1.00	0.00
117	SHS 160x10.0	123.22	-2079.93	5.13	0.90	0.97
Total Cost		3375.06				

Table 3.13: Results of topology optimization for SHS trusses with buckling curve b. C_0 = initial cost; C^* = minimum cost obtained; t^* = runtime when the optimum was found; t_{fin} = runtime at termination (time limit 21600 s); G_0 = initial optimality gap; G^* = optimality gap, when optimum was found; G_{fin} = final optimality gap.

i	C_0 [10^2 €]	C^* [10^2 €]	$\frac{C_0 - C^*}{C^*}$ [%]	t^* [s]	t_{fin}	G_0 [%]	G^* [%]	G_{fin} [%]
1	12.56	**12.00**	4.66	29	363	28.20	15.00	1.80
2	13.56	13.05	3.91	145	848	32.50	18.40	1.89
3	13.19	12.12	8.81	2922	4872	32.90	8.00	1.84
4	16.14	16.08	0.32	270	339	25.30	6.68	1.50
5	16.44	**15.56**	5.64	566	922	28.50	10.70	1.93
6	16.78	15.74	6.62	2517	7984	30.20	13.60	2.00
7	28.71	27.60	4.01	241	816	32.90	13.80	1.98
8	31.01	29.85	3.89	1301	1302	35.30	1.72	1.70
9	29.20	**27.47**	6.32	3398	3412	34.40	2.25	1.99
10	36.99	35.40	4.50	38	50	23.20	5.87	0.87
11	35.20	34.46	2.15	356	371	24.10	3.71	2.00
12	34.80	**33.64**	3.44	1075	1312	26.00	6.00	1.94

3.4 Summary of Topology Optimization

The results of topology optimization are summarized in Table 3.18. Note that for SHS trusses, the summary is based on the results obtained with buckling curve 'b'. The following observations can be made:

- Tubular trusses are 5–10% more economical than trusses with HEA/HEB chords and CHS braces
- The weight of the minimum cost tubular trusses is 4–8% greater, except for the 24 m span truss with $h = L/10$, where tubular truss is 6% lighter.

Table 3.18: Comparison of minimum cost HEA/HEB/CHS and SHS trusses. For SHS trusses, the results obtained using buckling curve 'b' are reported. Costs and weights are given for cost optimized trusses. In addition, the cost and weight ratios are reported.

L [m]	L/h	C_{HEA} [€]	C_{SHS} [€]	$\frac{C_{SHS}}{C_{HEA}}$	W_{HEA} [10^2 kg]	W_{SHS} [10^2 kg]	$\frac{W_{SHS}}{W_{HEA}}$
24	10	1336.96	1200.22	0.90	11.48	10.78	0.94
24	20	1636.08	1556.48	0.95	14.66	15.79	1.08
36	10	2972.95	2746.61	0.92	25.75	27.04	1.05
36	20	3598.56	3364.29	0.93	33.48	34.90	1.04

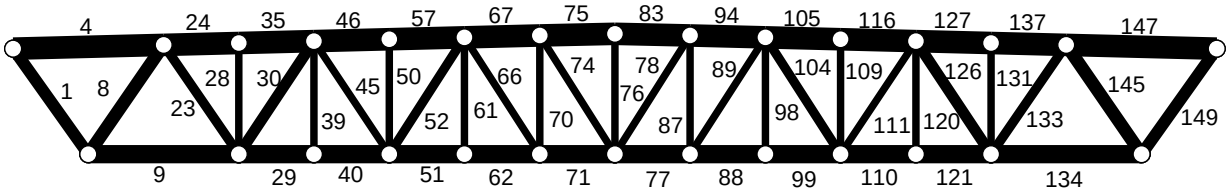

Figure 3.10: Optimum topology for SHS profiles with buckling curve 'b'. $L = 24\,\text{m}$, $h = L/10$. $C^* = 1200$€.

Table 3.14: Optimum SHS truss design for $L = 24\,\text{m}$, $h = L/10$ with buckling curve 'b'. The axial forces and design values of the bending moment are given. Furthermore, the utilization ratio for strength, U_S, and stability, U_B, are reported. Due to symmetry, only the members on the left to the symmetry axis are shown.

i	Profile	C [€]	N [kN]	M_{Ed} [kNm]	U_S	U_B
1	SHS 90x3.0	52.63	288.78	0.00	0.80	0.00
4	SHS 110x6.0	116.10	-167.91	20.51	0.28	0.75
8	SHS 100x3.0	60.14	-285.46	0.00	0.70	0.96
9	SHS 100x5.0	93.01	329.92	10.25	0.60	0.00
23	SHS 50x4.0	33.50	214.58	0.00	0.87	0.00
24	SHS 110x6.0	58.05	-451.88	5.13	0.50	0.59
28	SHS 40x3.0	18.89	-34.17	0.00	0.23	0.87
29	SHS 100x5.0	46.51	546.72	2.56	0.76	0.00
30	SHS 80x3.0	48.73	-171.23	0.00	0.54	0.92
35	SHS 110x6.0	58.05	-451.88	5.13	0.50	0.59
39	SHS 40x3.0	19.21	-0.00	0.00	0.00	0.00
40	SHS 100x5.0	46.51	546.72	2.56	0.76	0.00
45	SHS 40x3.0	23.09	125.22	0.00	0.84	0.00
46	SHS 110x6.0	58.05	-616.37	5.13	0.68	0.81
50	SHS 40x3.0	19.53	-34.17	0.00	0.23	0.92
51	SHS 100x5.0	46.51	661.35	2.56	0.93	0.00
52	SHS 60x3.0	36.75	-83.33	0.00	0.36	0.94
57	SHS 110x6.0	58.05	-616.37	5.13	0.68	0.81
61	SHS 40x3.0	19.85	0.00	0.00	0.00	0.00
62	SHS 100x5.0	46.51	661.35	2.56	0.93	0.00
66	SHS 40x3.0	23.63	40.66	0.00	0.27	0.00
67	SHS 110x6.0	58.05	-683.61	5.13	0.75	0.89
70	SHS 40x3.0	20.17	-34.17	0.00	0.23	0.97
71	SHS 100x5.0	46.51	683.40	2.56	0.96	0.00
74	SHS 40x3.0	23.90	-0.00	0.00	0.00	0.00
75	SHS 110x6.0	58.05	-683.61	5.13	0.75	0.89
76	SHS 40x3.0	10.25	-0.00	0.00	0.00	0.00
Total Cost		1200.22				

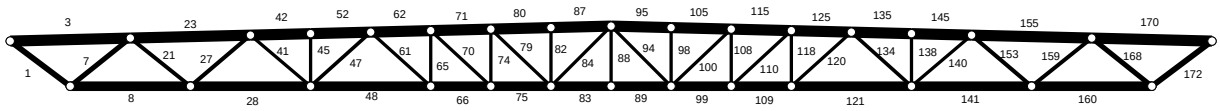

Figure 3.11: Optimum topology for SHS profiles with buckling curve 'b'. $L = 24\,\text{m}$, $h = L/20$. $C^* = 1566\,€$.

Table 3.15: Optimum SHS truss design for $L = 24\,\text{m}$, $h = L/20$ with buckling curve 'b'. The axial forces and design values of the bending moment are given. Furthermore, the utilization ratio for strength, U_S, and stability, U_B, are reported. Due to symmetry, only the members on the left to the symmetry axis are shown.

i	Profile	C [€]	N [kN]	M_{Ed} [kNm]	U_S	U_B
1	SHS 110x4.0	44.71	396.81	0.00	0.68	0.00
3	SHS 120x10.0	141.87	-317.55	13.13	0.22	0.32
7	SHS 90x4.0	37.03	-381.13	0.00	0.80	0.92
8	SHS 120x8.0	122.22	615.06	6.56	0.48	0.00
21	SHS 50x5.0	22.00	273.16	0.00	0.92	0.00
23	SHS 120x10.0	141.87	-828.62	13.13	0.57	0.85
27	SHS 80x3.0	28.38	-263.48	0.00	0.82	0.98
28	SHS 120x8.0	122.22	1029.12	6.56	0.80	0.00
41	SHS 50x3.0	17.18	186.92	0.00	0.97	0.00
42	SHS 120x10.0	70.94	-1171.91	3.28	0.72	0.77
45	SHS 50x3.0	11.46	-27.34	0.00	0.14	0.18
47	SHS 50x4.0	20.47	-140.10	0.00	0.57	0.98
48	SHS 120x8.0	122.22	1275.68	6.56	0.99	0.00
52	SHS 120x10.0	70.94	-1171.91	3.28	0.72	0.77
61	SHS 50x3.0	17.61	92.77	0.00	0.48	0.00
62	SHS 120x10.0	70.94	-1345.06	3.28	0.82	0.88
65	SHS 50x3.0	12.11	-62.06	0.00	0.32	0.41
66	SHS 120x8.0	61.11	1344.64	1.64	0.97	0.00
70	SHS 50x3.0	17.83	49.79	0.00	0.26	0.00
71	SHS 120x10.0	70.94	-1381.62	3.28	0.84	0.91
74	SHS 50x3.0	12.44	-33.81	0.00	0.18	0.23
75	SHS 120x8.0	61.11	1381.19	1.64	1.00	0.00
79	SHS 50x3.0	18.06	9.16	0.00	0.05	0.00
80	SHS 120x10.0	70.94	-1388.26	3.28	0.85	0.91
82	SHS 50x3.0	12.76	-27.34	0.00	0.14	0.19
83	SHS 120x8.0	61.11	1366.80	1.64	0.99	0.00
84	SHS 50x3.0	18.52	29.74	0.00	0.15	0.00
87	SHS 120x10.0	70.94	-1388.26	3.28	0.85	0.91
88	SHS 50x3.0	6.55	0.00	0.00	0.00	0.00
Total Cost		1556.48				

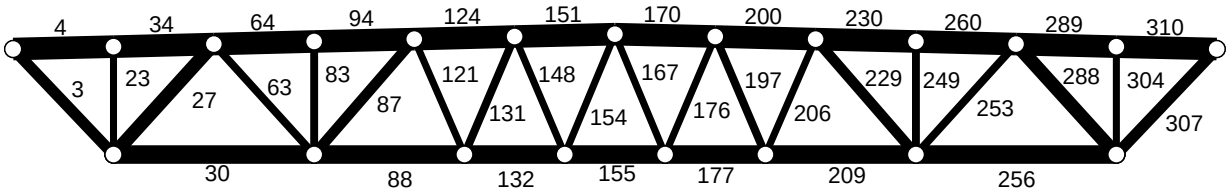

Figure 3.12: Optimum topology for SHS profiles with buckling curve 'b'. $L = 36\,\text{m}$, $h = L/10$. $C^* = 2747\,€$.

Table 3.16: Optimum SHS truss design for $L = 36\,\text{m}$, $h = L/10$ with buckling curve 'b'. The axial forces and design values of the bending moment are given. Furthermore, the utilization ratio for strength, U_S, and stability, U_B, are reported. Due to symmetry, only the members on the left to the symmetry axis are shown.

i	Profile	C [€]	N [kN]	M_{Ed} [kNm]	U_S	U_B
3	SHS 110x4.0	129.65	506.99	0.00	0.86	0.00
4	SHS 150x8.0	195.93	-349.76	20.51	0.23	0.34
23	SHS 60x3.0	42.83	-68.34	0.00	0.29	0.99
27	SHS 120x5.0	168.05	-403.80	0.00	0.51	0.98
30	SHS 120x8.0	305.55	621.27	41.00	0.99	0.00
34	SHS 150x8.0	195.93	-349.76	20.51	0.23	0.34
63	SHS 60x4.0	69.28	295.55	0.00	0.97	0.00
64	SHS 150x8.0	195.93	-820.34	20.51	0.54	0.80
83	SHS 60x4.0	52.43	-68.34	0.00	0.23	0.86
87	SHS 100x4.0	123.22	-199.24	0.00	0.38	0.97
88	SHS 120x8.0	229.16	950.82	23.06	0.98	0.00
94	SHS 150x8.0	195.93	-820.34	20.51	0.54	0.80
121	SHS 60x3.0	49.96	84.94	0.00	0.36	0.00
124	SHS 150x8.0	195.93	-984.99	20.51	0.65	0.95
131	SHS 80x3.0	69.04	-84.65	0.00	0.26	0.73
132	SHS 120x8.0	152.78	1017.83	10.25	0.84	0.00
148	SHS 60x3.0	50.88	9.38	0.00	0.04	0.00
151	SHS 150x8.0	195.93	-1021.82	20.51	0.68	0.99
154	SHS 60x3.0	51.80	-9.35	0.00	0.04	0.19
155	SHS 120x8.0	76.39	1025.10	10.25	0.84	0.00
Total Cost		2746.61				

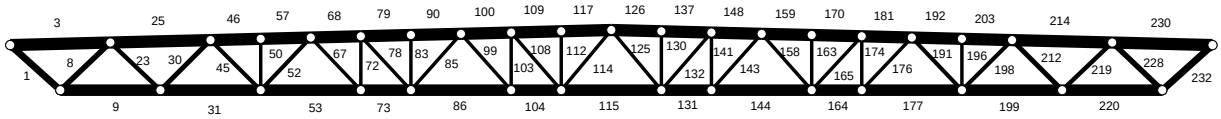

Figure 3.13: Optimum topology for SHS profiles with buckling curve 'b'. $L = 36\,\text{m}$, $h = L/20$. $C^* = 3364$€.

Table 3.17: Optimum SHS truss design for $L = 36\,\text{m}$, $h = L/20$ with buckling curve 'b'. The axial forces and design values of the bending moment are given. Furthermore, the utilization ratio for strength, U_S, and stability, U_B, are reported. Due to symmetry, only the members on the left to the symmetry axis are shown.

i	Profile	C [€]	N [kN]	M_{Ed} [kNm]	U_S	U_B
1	SHS 140x5.0	89.51	546.68	0.00	0.58	0.00
3	SHS 160x10.0	246.43	-406.47	20.51	0.20	0.27
8	SHS 100x5.0	64.15	-530.98	0.00	0.81	0.99
9	SHS 150x10.0	229.09	791.31	10.25	0.39	0.00
23	SHS 70x5.0	43.43	407.07	0.00	0.93	0.00
25	SHS 160x10.0	246.43	-1086.77	20.51	0.52	0.71
30	SHS 100x4.0	57.17	-396.50	0.00	0.75	0.92
31	SHS 150x10.0	229.09	1366.80	10.25	0.67	0.00
45	SHS 60x5.0	37.45	306.44	0.00	0.83	0.00
46	SHS 160x10.0	123.22	-1583.98	5.13	0.69	0.73
50	SHS 60x3.0	20.42	-34.17	0.00	0.15	0.20
52	SHS 90x3.0	44.35	-252.05	0.00	0.70	0.90
53	SHS 150x10.0	229.09	1757.31	10.25	0.86	0.00
57	SHS 160x10.0	123.22	-1583.98	5.13	0.69	0.73
67	SHS 60x3.0	28.89	194.24	0.00	0.83	0.00
68	SHS 160x10.0	123.22	-1891.86	5.13	0.82	0.87
72	SHS 60x3.0	21.42	-140.65	0.00	0.60	0.84
73	SHS 150x10.0	114.54	1891.27	2.56	0.87	0.00
78	SHS 60x3.0	29.25	142.13	0.00	0.61	0.00
79	SHS 160x10.0	123.22	-1988.69	5.13	0.86	0.91
83	SHS 60x3.0	21.91	-34.17	0.00	0.15	0.21
85	SHS 60x3.0	29.99	-93.51	0.00	0.40	0.79
86	SHS 150x10.0	229.09	2050.20	10.25	1.00	0.00
90	SHS 160x10.0	123.22	-1988.69	5.13	0.86	0.91
99	SHS 60x3.0	29.99	44.72	0.00	0.19	0.00
100	SHS 160x10.0	123.22	-2080.56	5.13	0.90	0.96
103	SHS 60x3.0	22.91	-33.43	0.00	0.14	0.21
104	SHS 150x10.0	114.54	2079.91	2.56	0.96	0.00
108	SHS 60x3.0	30.36	-0.96	0.00	0.00	0.01
109	SHS 160x10.0	123.22	-2079.93	5.13	0.90	0.96
112	SHS 60x3.0	23.41	-34.17	0.00	0.15	0.22
114	SHS 60x3.0	31.12	45.43	0.00	0.19	0.00
115	SHS 150x10.0	114.54	2050.20	10.25	1.00	0.00
117	SHS 160x10.0	123.22	-2079.93	5.13	0.90	0.96
Total Cost		3364.29				

References

EN 1990 (2002), *Eurocode – Basis of structural design*, CEN.

EN 1993–1–1 (2005), *Eurocode 3: Design of Steel Structures. Part 1-1: General rules and rules for buildings*, CEN.

EN 1993–1–8 (2005), *Eurocode 3: Design of Steel Structures. Part 1-8: Design of joints*, CEN.

4 Resistance checks of members and joints

4.1 Introduction

In the previous optimization the mechanical models of the trusses were based on the traditional truss analysis. This means that in the structural analysis the members are modeled using hinge ended members, both the chords and the braces, see *Fig.* 4.1. The additioanl moments were added to the chords and their resistances were checked using the interaction formula of the axial load and the moment following EN 1993-1-1. The resistances of the braces were checked only for the axial load. The buckling lengths of the compressed members were derived using the buckling lengths 0.9 times the system lengths and the system lengths were the lengths between adjacent hinges. No eccentricities at the joints were modeled, and the resistances of the joints were not checked. Only design rule of the joints which was embedded in the topology optimization was the rule, that the brace shall not meet the chord in the angle less than 30 degrees.

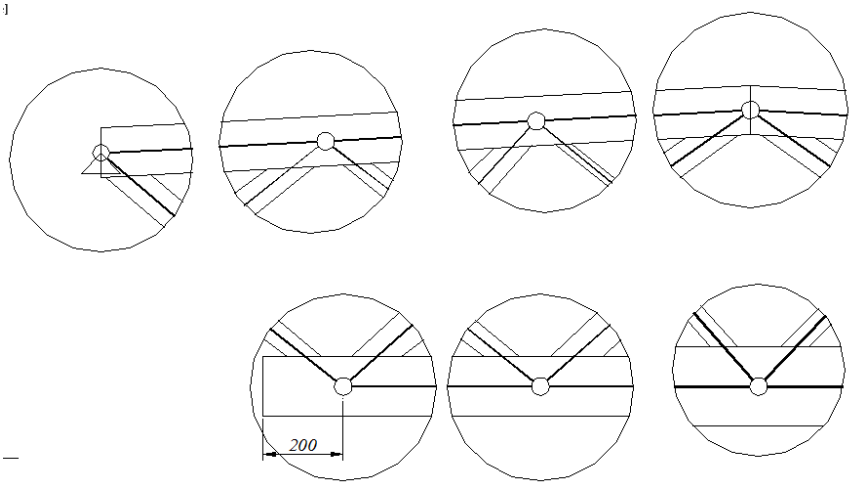

Figure 4.1. Local joints models, traditional truss analysis.

In this chapter the results of the previous chapters are evaluated against all requirements of EN 1993-1-8 concerning with the structural model and the corresponding resistances of the members and joints. The verification is done in the following steps:

1. The resistance checks of the **members** using the frame analysis model for the optimized trusses. The frame analysis model here means that the chords were modeled as continuous members, but the braces are hinge ended members without eccentricity. The frame analysis model means the use of beam elements including shear deformations. To do this the input data from the optimization results was made such that the frame analysis program could read the data: nodes, members, materials, supports and loads.
2. The resistance checks of the **members and the joints** using the frame analysis model with the eccentricity elements at the ends of the braces formulated using the principles of *Fig. 4.2*. The chords were modeled as continuous members (as in the previous step) and the braces were modeled as hinge ended members. Using this model the eccentricity moments of the joints will be transmitted to chords, both to the top chord and to the bottom chord, based on the principles of the finite element method, meaning with respect to the bending

stiffness *I*/*L* of the chord members, where *I* is the moment of inertia of the member and *L* is the system length of the chord member connected at the joint. To do this the analysis model had to be generated from the actual geometrical model including the gaps at the joints. Only gap joints were considered. A special program was done to this generation starting at the results of the optimization.

- Constant gap 40 mm was used for HEB/HEA trusses and the minimum allowed gap based on EN 1993-1-8 was used for the tubular trusses.
- It is possible to design the trusses without eccentricities at the joints. Then overlapped joints should be used in many cases. Overlapped joints are much more complicated in the fabrication, so the gap joints are preferred by the fabricators. When using gap joints, then it is almost impossible to prevent the eccentricities, especially when the constant gap is used, as preferred by the fabricators who use manual assembly techniques. In the automatized robot-fabrication the variations of gaps do not mean extra costs, but this kind of technology is not yet used in the fabrication of trusses, at least not in Finland. In this study, only gap joints are considered.
- The major difference between the models of *Figs.* 1 and 2 is that the models of *Fig.* 1 can be constructed without the information of the details of the joints. When constructing the models of *Fig.* 2, the detailed information about the joints should be available. Here the weakness of the models of *Fig.* 1 can be seen: Using these models the exact design of the members and the joints cannot be performed.
  - The effect of different models to the design of the members is not very critical. The largest difference is at the lengths of the braces and the changes at the lengths are not very large. At the chords the moment effect was taken into account approximatively.
  - The design of joints can be done and have been done (Jalkanen, 2009) using the models of *Fig*. 1. The accuracy of that technics is open and it will not be considered in this study.
  - It is clear that the global structural analysis models are different when using the models of *Figs*. 1 and 2. In previous studies has been shown that if the truss is composed from "triangular base forms" then the axial forces of the members do not change very much. Vierendeel typed trusses, or the trusses which have Vierendeel typed parts are not considered here. Rather open question is: What are the effects of eccentricity moments to the design of members and joints? This question will be studied in this research.

3. At this step the resistances of **the braces and the joints** were checked after transmitting the eccentricity moments of the joints to the braces following the clause 5.1.5(7) of EN 1993-1-8: *When the eccentricities are outside the limits given in 5.1.5(5), the moments resulting from the eccentricities should be taken into account in the design of the joints all members (see Ammendment of EN 1993-1-8, 2009). In this case the moments produced by the eccentricity should be distributed between all the members meeting at the joint, on the basis of their relative stiffness coefficients I/L.* This was done for the joints where the limits of the clause 5.1.5(5) of EN 1993-1-8 were exceeded. After this step can be concluded that all requirements of the Eurocodes have been checked. The resistances of the chords were

checked in the previous step in all cases, not only for the cases where these limits were exceeded. The resistance checks for the chords were somewhat conservative, because the eccentricity moment was distributed just for the chords.

4. At the last step the estimations of the optimized trusses due to the previous steps are given to complete the final results to evaluate the trusses with different steel profiles. This estimation will be done by **reviewing utility ratios of the members and the joints after each step**. The members are the same at each step originating from the optimization.

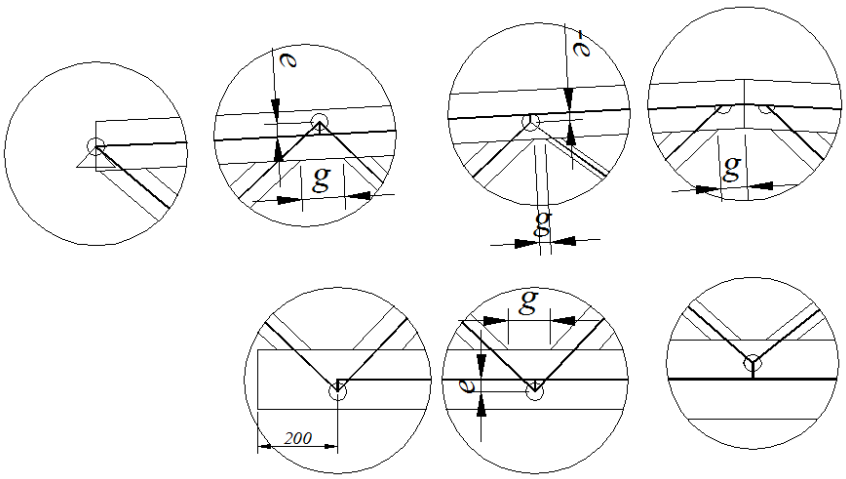

Figure 4.2. Local analysis models with eccentricities in frame analysis.

The motivation to the described evaluation is:

- To verify the results of the optimization, because the used optimization routine did not include all requirements of the Eurocodes;
- To get the information to estimate the results of the huge number optimizations which are available in the literature concerned with the optimization of the trusses using the traditional truss analysis, local models of *Fig.* 1. The information means here: how well the results of the traditional truss analysis complete all requirements of the present Eurocodes?

The structural analysis program which was used in the steps 1-3 was *Autodesk ® Robot ™ Structural Analysis Professional*. The resistances of the members were checked using the same program and the resistances of the joints were checked using the in-house Excel.

4.2 Notations

There are two types of trusses which have been optimized in the previous chapters:

- HEA/HEB chords with circular hollow section (CHS) braces: called HEA truss in this chapter;
- Square hollow section (SHS) chords and braces: called SHS truss in this chapter.

Both truss types have been optimized with two heights $L/10$ and $L/20$ and with two spans L = 24 and 36 m. Totally we have eight trusses. The following notation is used for the trusses:

- HEA_24_10;

- HEA_24_20;
- HEA_36_10;
- HEA_36_20
- SHS_24_10;
- SHS_24_20;
- SHS_36_10;
- SHS_36_20.

4.3 Step 1

4.3.1 HEA_24_10

Fig. 3.2 illustrates the optimized truss HEA_24_10. *Fig.* 4.3 shows the Robot model at the step 1.

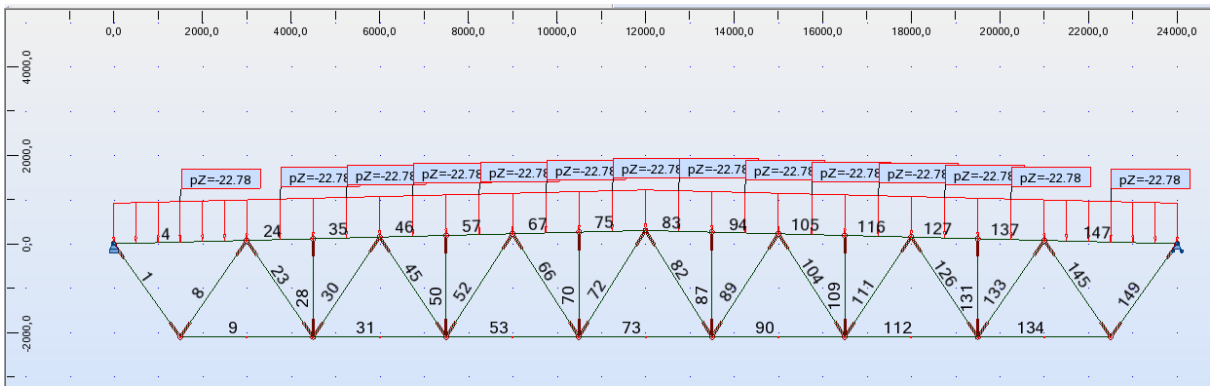

Figure 4.3. Robot model of HEA_24_10 at step 1.

The utility ratios of the members are shown in Table 4.1.

Table 4.1. Utility ratios of the members for HEA_24_10 at step 1. Lay and Laz are the buckling lengths of the members in cm.

Member	Section	Material	Lay (cm)	Laz (cm)	Ratio
1	PIPE_4	S355	118.31	131.46	0.97
4	HEB 100	S460	65.00	118.39	0.63
8	PIPE_7	S355	81.19	90.21	1.00
9	HEA 100	S460	66.58	119.51	0.35
23	PIPE_3	S355	119.16	132.40	0.79
24	HEB 100	S460	32.50	59.20	0.81
28	PIPE_2	S355	124.06	137.84	0.31
30	PIPE_6	S355	80.99	89.99	0.93
31	HEA 100	S460	66.58	119.51	0.56
35	HEB 100	S460	32.50	59.20	0.56
45	PIPE_2	S355	151.63	168.47	0.79
46	HEB 100	S460	32.50	59.20	0.71
50	PIPE_2	S355	128.26	142.51	0.61
52	PIPE_5	S355	97.54	108.38	0.69
53	HEA 100	S460	66.58	119.51	0.68
57	HEB 100	S460	32.50	59.20	0.68
66	PIPE_1	S355	229.67	255.19	0.34

67	HEB 100	S460	32.50	59.20	0.74
70	PIPE_2	S355	132.47	147.19	0.72
72	PIPE_1	S355	234.92	261.03	0.39
73	HEA 100	S460	66.58	119.51	0.70
75	HEB 100	S460	32.50	59.20	0.73

It can be seen, that the maximum utility factor of the top chord (HEB100) is 0.81 (member 24) and the maximum utility ratio of the bottom chord (HEA100) is 0.70 (member 73). This means that the moments added in the optimization ($qL^2/10$ and $qL^2/20$) to the chords overestimate the moments of the chords if the joints are designed without eccentricities. The maximum utility of the braces is 1.00 (member 8).

4.3.2 HEA_24_20

Fig. 3.3 illustrates the optimal truss HEA_24_20. The Robot model of this truss is in *Fig.* 4.4.

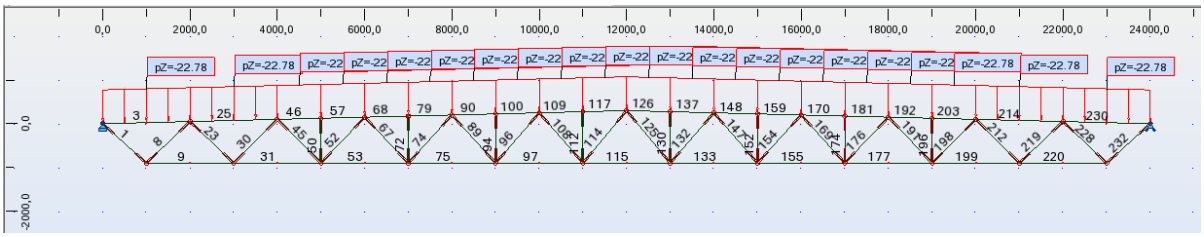

Figure 4.4. Robot model of HEA_24_20 at step 1.

The utility ratios of the members are shown in Table 4.2.

Table 4.2. Utility ratios of the members for HEA_24_20 at step 1.

Member	**Section**	**Material**	**Lay (cm)**	**Laz (cm)**	**Ratio**
1	PIPE_5	S355	48.87	54.30	0.76
3	HEB 120	S460	35.71	65.47	0.30
8	PIPE_5	S355	50.10	55.67	0.96
9	HEB 120	S460	35.70	65.45	0.34
23	PIPE_5	S355	50.10	55.67	0.54
25	HEB 120	S460	35.71	65.47	0.61
30	PIPE_6	S355	42.36	47.06	0.84
31	HEB 120	S460	35.70	65.45	0.58
45	PIPE_4	S355	64.83	72.04	0.63
46	HEB 120	S460	17.86	32.74	0.76
50	PIPE_1	S355	85.08	94.53	0.19
52	PIPE_4	S355	66.48	73.86	0.92
53	HEB 120	S460	35.70	65.45	0.75
57	HEB 120	S460	17.86	32.74	0.76
67	PIPE_3	S355	82.98	92.20	0.61
68	HEB 120	S460	17.86	32.74	0.92
72	PIPE_1	S355	89.23	99.15	0.14
74	PIPE_4	S355	68.15	75.73	0.57
75	HEB 120	S460	35.70	65.45	0.84
79	HEB 120	S460	17.86	32.74	0.92
89	PIPE_1	S355	123.40	137.11	0.47

90	HEB 120	S460	17.86	32.74	0.98
94	PIPE_1	S355	93.38	103.76	0.23
96	PIPE_2	S355	85.45	94.95	0.52
97	HEB 120	S460	35.70	65.45	0.88
100	HEB 120	S460	17.86	32.74	1.00
108	PIPE_1	S355	126.50	140.55	0.15
109	HEB 120	S460	17.86	32.74	1.01
112	PIPE_1	S355	97.53	108.37	0.21
114	PIPE_1	S355	129.66	144.07	0.16
115	HEB 120	S460	35.70	65.45	0.87
117	HEB 120	S460	17.86	32.74	0.99

In this case the maximum utility ratio of the top chord is very near by 1.00 (in one member 1.01) so the additional moment $qL^2/10$ works well in this case. The maximum utility at the bottom chord is 0.87 (member 115) so the additional moment of the bottom chord is a little bit too large. There exists moment at the bottom chord allthough there are no eccentricities. This moment is originating from the deflection of the entire truss, which bends the bottom chord, so there should be some extra moment at the bottom chord. This can be seen in *Fig.* 4.5.

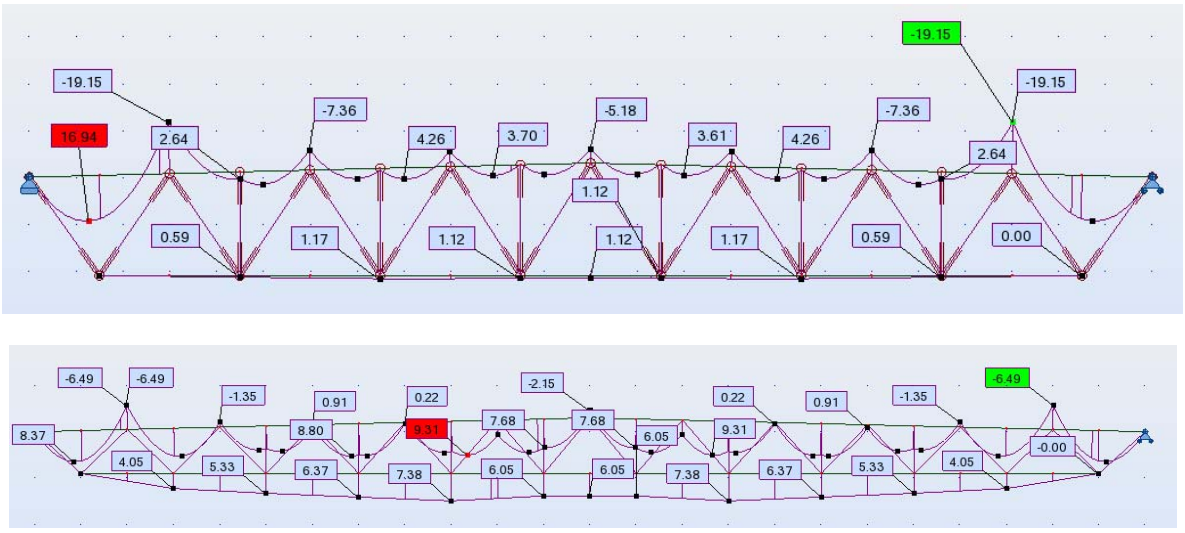

Figure 4.5. Bending moments of trusses HEA_24_20 and HEA_24_10.

4.3.3 HEA_36_10

Fig. 3.4 illustrates the optimal truss HEA_36_10. The Robot model of this truss is in *Fig.* 4.6.

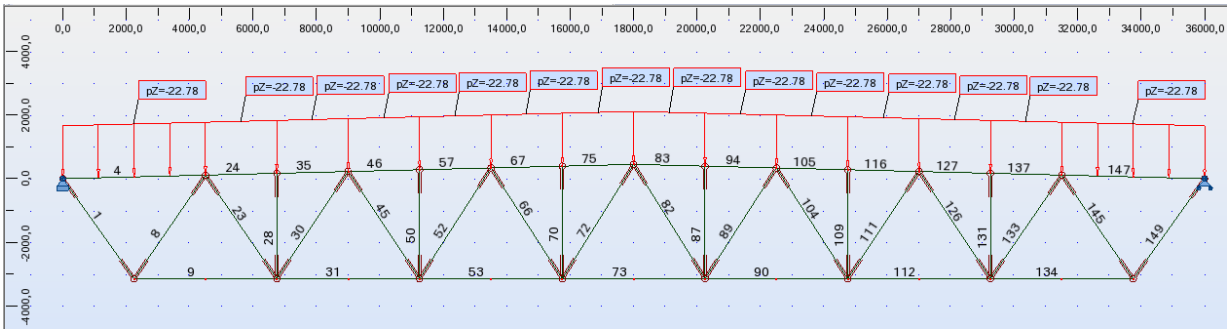

Figure 4.6. Robot model of HEA_36_10 at step 1.

The utility ratios of the members are shown in Table 4.3.

Table 4.3. Utility ratios of the members for HEA_36_10 at step 1.

Member	Section	Material	Lay (cm)	Laz (cm)	Ratio
1	PIPE_4	S355	140.60	156.23	0.91
4	HEA 160	S460	61.67	112.97	0.59
8	PIPE_8	S355	75.54	83.94	0.86
9	HEA 140	S460	70.62	127.83	0.35
23	PIPE_5	S355	118.70	131.88	0.78
24	HEA 160	S460	30.84	56.49	0.79
28	PIPE_3	S355	152.15	169.05	0.31
30	PIPE_7	S355	83.90	93.23	1.01
31	HEA 140	S460	70.62	127.83	0.57
35	HEA 160	S460	30.84	56.49	0.56
45	PIPE_2	S355	232.14	257.93	0.90
46	HEA 160	S460	30.84	56.49	0.71
50	PIPE_3	S355	157.31	174.79	0.61
52	PIPE_6	S355	107.73	119.70	0.98
53	HEA 140	S460	70.62	127.83	0.69
57	HEA 160	S460	30.84	56.49	0.68
66	PIPE_1	S355	344.50	382.78	0.49
67	HEA 160	S460	30.84	56.49	0.74
70	PIPE_3	S355	162.46	180.52	0.73
72	PIPE_1	S355	352.39	391.54	1.33
73	HEA 140	S460	70.62	127.83	0.71
75	HEA 160	S460	30.84	56.49	0.71

The utilities of the chords, and the corresponding conclusions, are very similar to those of the truss HEA_24_10. One special issue can be seen at the brace 72. The traditional truss analysis give for this member the axial force 0, see Table 3.5, member 72, and the smallest cross-section of the catalogue is chosen, see Table 2.2: D33.7x3.2. Using the frame analysis small compressive force 6.2 kN is acting at that member. The slenderness of the member is 352 and the program give a warning because allowed slendeness in the program is 210, set by the dealer of the program. The program calculates the utility ratio (using buckling length 0.9 times the system length, as given for this case, not 0.75 times the buckling length as could be used) 1.33 for this member. So, in reality this member should be larger.

4.3.4 HEA_36_20

Fig. 3.5 illustrates the optimal truss HEA_36_20. The Robot model of this truss is in *Fig.* 4.7.

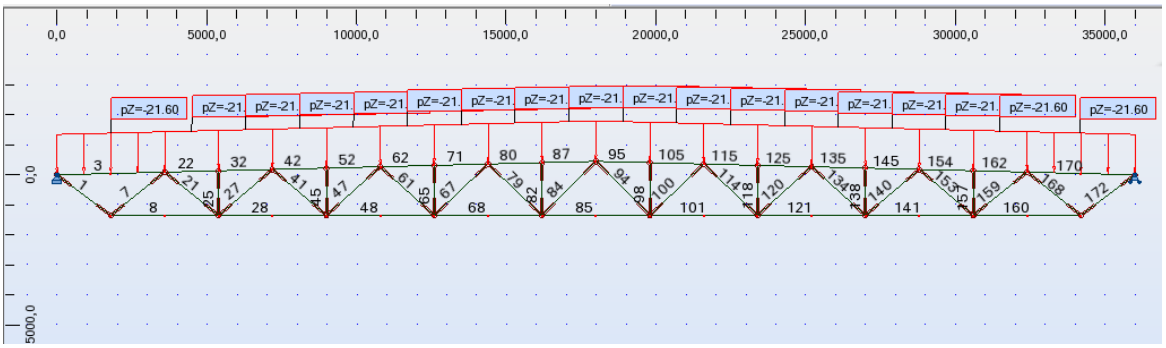

Figure 4.7. Robot model of HEA_36_20 at step 1.

The utility ratios of the members are shown in Table 4.4.

Table 4.4. Utility ratios of the members for HEA_36_20 at step 1.

Member	Section	Material	Lay (cm)	Laz (cm)	Ratio
1	PIPE_8	S355	52.35	52.35	0.95
3	HEB 160	S460	47.82	80.05	0.37
7	PIPE_9	S355	43.53	43.53	0.91
8	HEB 160	S460	47.81	80.03	0.36
21	PIPE_5	S355	83.73	83.73	0.79
22	HEB 160	S460	23.91	40.03	0.62
25	PIPE_2	S355	83.27	83.27	0.15
27	PIPE_7	S355	58.32	58.32	0.91
28	HEB 160	S460	47.81	80.03	0.59
32	HEB 160	S460	23.91	40.03	0.58
41	PIPE_4	S355	108.30	108.30	0.82
42	HEB 160	S460	23.91	40.03	0.78
45	PIPE_2	S355	88.31	88.31	0.27
47	PIPE_6	S355	72.53	72.53	0.99
48	HEB 160	S460	47.81	80.03	0.73
52	HEB 160	S460	23.91	40.03	0.78
61	PIPE_2	S355	135.78	135.78	0.76
62	HEB 160	S460	23.91	40.03	0.89
65	PIPE_2	S355	93.36	93.36	0.32
67	PIPE_3	S355	111.97	111.97	1.03
68	HEB 160	S460	47.81	80.03	0.78
71	HEB 160	S460	23.91	40.03	0.90
79	PIPE_1	S355	206.08	206.08	0.05
80	HEB 160	S460	23.91	40.03	0.93
82	PIPE_2	S355	98.40	98.40	0.32
84	PIPE_1	S355	211.30	211.30	0.21
85	HEB 160	S460	47.81	80.03	0.78
87	HEB 160	S460	23.91	40.03	0.91

The maximum utility of the top chord is in this case 0.93 and at the bottom chord 0.78, so the additional moment $qL^2/20$ of the bottom chord is a little bit conservative in this case. The maximum utility ratio of the braces is 1.03 at the brace 67. Using the traditional truss analysis the axial force of the member 67 is 75.6 kN and the utility ratio is 0.92. Using the frame analysis the axial force of

the member 67 is 84.3 kN and the utility ratio is 1.03. The buckling lenghts in both analyses are the same. This difference 100x(75.6-84.3)/75.6 = -11.5 % was largest which was found giving larger values for axial forces using the frame analysis than the traditional truss analysis. Minus sign means that the axial force using the frame analysis is larger than using the traditional truss analysis. Table 4.5 illustrates the differences for this truss.

Table 4.5. Axial forces of the truss HEA_36_20 and their differences in percents.

Member	Truss theory (kN)	Frame theory (kN)	Difference (%)
1	595	574	3,57
3	-476	-460	3,39
7	-572	-547	4,25
8	923	887	3,90
21	442	386	12,51
22	-1268	-1190	6,17
25	-41	-11	73,31
27	-363	-359	0,88
28	1544	1462	5,28
32	-1268	-1189	6,22
41	280	250	10,77
42	-1758	-1654	5,90
45	-41	-18	55,28
47	-210	-213	-1,24
48	1914	1811	5,36
52	-1758	-1654	5,93
61	139	114	18,23
62	-2018	-1897	5,98
65	-41	-20	50,24
67	-76	-84	-11,48
68	2072	1957	5,56
71	-2018	-1896	6,01
79	14	5	62,64
80	-2082	-1962	5,80
82	-41	-19	53,57
85	45	23	47,92
85	2050	1944	5,18
87	-2082	-1961	5,82

It can be seen, that large differences occur at the members where are small axial forces but with large forces the differences are not large. For most of the members the axial loads are conservative using the traditional truss analysis compared to the results of the frame analysis, but for all members.

4.3.5 SHS_24_10

Fig. 3.10 illustrates the optimal truss SHS_24_10. The Robot model of this truss is in *Fig.* 4.8.

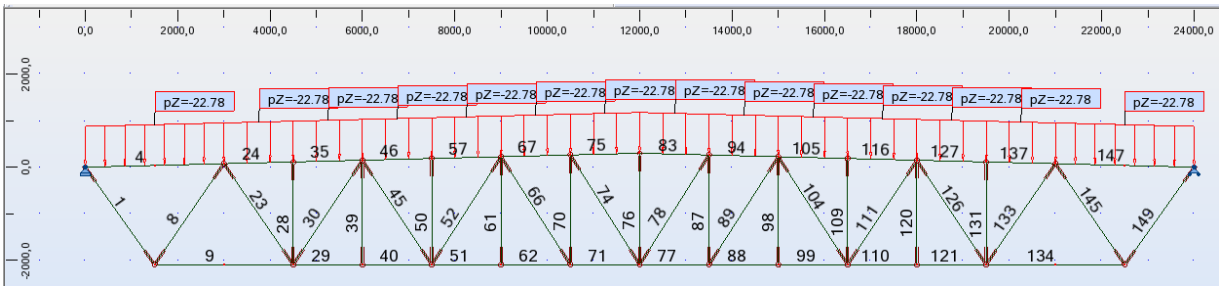

Figure 4.8. Robot model of SHS_24_10 at step 1.

The utility ratios of the members are shown in Table 4.6.

Table 4.6. Utility ratios of the members for SHS_24_10 at step 1.

Member	Section	Material	Lay (cm)	Laz (cm)	Ratio
1	RRHS 90x90x3	S355	65.82	73.14	0.82
4	RRHS 110x110x6	S420	64.18	71.31	0.78
8	RRHS 100x100x3	S355	60.35	67.05	0.99
9	RRHS 100x100x5	S420	70.35	78.17	0.44
23	RHS 50x50x4	S355	128.63	142.97	0.80
24	RRHS 110x110x6	S420	32.09	35.66	0.99
28	RHS 40x40x3	S355	133.77	148.65	0.36
29	RRHS 100x100x5	S420	35.18	39.09	0.71
30	RRHS 80x80x3	S355	77.96	86.63	0.96
35	RRHS 110x110x6	S420	32.09	35.66	0.67
39	RHS 40x40x3	S355	136.04	151.17	0.01
40	RRHS 100x100x5	S420	35.18	39.09	0.71
45	RHS 40x40x3	S355	163.50	181.68	0.80
46	RRHS 110x110x6	S420	32.09	35.66	0.86
50	RHS 40x40x3	S355	138.31	153.69	0.72
51	RRHS 100x100x5	S420	35.18	39.09	0.86
52	RRHS 60x60x3	S355	108.06	120.07	0.99
57	RRHS	S420	32.09	35.66	0.80

	110x110x6				
61	RHS 40x40x3	S355	140.58	156.21	0.00
62	RRHS 100x100x5	S420	35.18	39.09	0.86
66	RHS 40x40x3	S355	167.29	185.90	0.26
67	RRHS 110x110x6	S420	32.09	35.66	0.88
70	RHS 40x40x3	S355	142.84	158.73	0.89
71	RRHS 100x100x5	S420	35.18	39.09	0.88
74	RHS 40x40x3	S355	169.20	188.02	0.01
75	RRHS 110x110x6	S420	32.09	35.66	0.87
76	RHS 40x40x3	S355	145.11	161.25	0.11

The utility ratios of the chords are a little bit larger than for the HEA_24_10 truss.

4.3.6 SHS_24_20

Fig. 3.11 illustrates the optimal truss SHS_24_20. The Robot model of this truss is in *Fig.* 4.9.

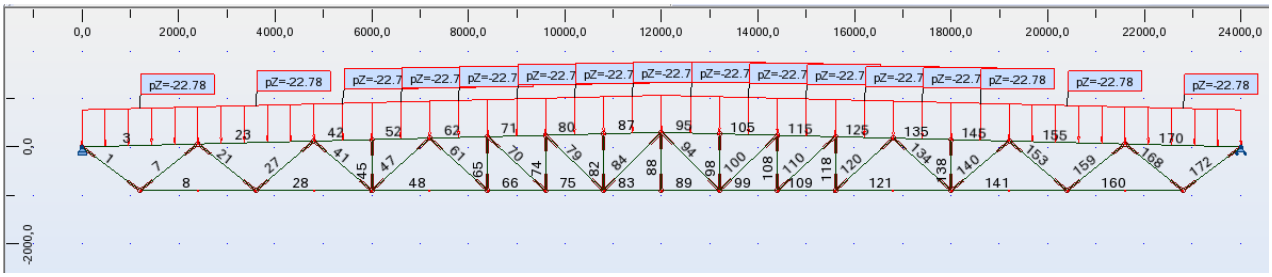

Figure 4.9. Robot model of SHS_24_20 at step 1.

The utility ratios of the members are shown in Table 4.7.

Table 4.7. Utility ratios of the members for SHS_24_20 at step 1.

Member	Section	Material	Lay	Laz	Ratio
1	RRHS 110x110x4	S355	31.35	34.83	0.70
3	SHS 120x120x10	S420	49.38	54.86	0.42
7	RRHS 90x90x4	S355	39.63	44.03	0.94
8	RRHS 120x120x8	S420	48.12	48.12	0.44
21	RHS 50x50x5	S355	76.88	85.44	0.90
23	SHS 120x120x10	S420	49.38	54.86	0.84

27	RRHS 80x80x3	S355	45.41	50.45	0.96
28	RRHS 120x120x8	S420	48.12	48.12	0.73
41	RRHS 50x50x3	S355	74.66	82.95	0.92
42	SHS 120x120x10	S420	24.69	27.43	0.81
45	RRHS 50x50x3	S355	49.78	55.31	0.11
47	RHS 50x50x4	S420	78.60	87.36	0.95
48	RRHS 120x120x8	S420	48.12	48.12	0.90
52	SHS 120x120x10	S420	24.69	27.43	0.83
61	RRHS 50x50x3	S355	76.53	85.04	0.47
62	SHS 120x120x10	S420	24.69	27.43	0.94
65	RRHS 50x50x3	S355	52.62	58.47	0.39
66	RRHS 120x120x8	S420	24.06	24.06	1.49
70	RRHS 50x50x3	S355	77.49	86.10	0.26
71	SHS 120x120x10	S420	24.69	27.43	0.97
74	RRHS 50x50x3	S355	54.04	60.05	0.24
75	RRHS 120x120x8	S420	24.06	24.06	2.96
79	RRHS 50x50x3	S355	78.46	87.18	0.05
80	SHS 120x120x10	S420	24.69	27.43	0.97
82	RRHS 50x50x3	S355	55.46	61.63	0.15
83	RRHS 120x120x8	S420	24.06	24.06	2.14
84	RRHS 50x50x3	S355	80.45	89.39	0.11
87	SHS 120x120x10	S420	24.69	27.43	0.95
88	RHS 40x40x3	S355	72.56	80.62	0.02

In this case very large utility ratios, maximum 2.96 at the member 75, can be seen at the bottom flange. In Robot resistance check of this mebmer the reference is given to the clause 6.2.9(2) of EN 1993-1-1. The proper reference is 6.2.9(5) and the Eq. 6.39 of EN 1993-1-1. This equation means the moment resistance of the cross-section resistance with bending moment and axial force:

$$M_{N,Rd} = M_{pl,Rd} \cdot \left(1 - \frac{N_{Ed}}{N_{pl,Rd}}\right) / \left(1 - \frac{A - 2bt}{2A}\right) but \ \frac{A - 2bt}{A} \leq 0.5 \qquad (4.1)$$

In this case for SHS120x120x8, f_y = 420 MPa and with the axial force N_{Ed} = 1365 kN in Robot:

$$A = 3364\,mm^2$$

$$W_{pl} = 137810\,mm^3$$

$$N_{pl,Rd} = 3364 \cdot 420 / 1000 = 1413\,kN$$

$$M_{pl,Rd} = 137810 \cdot 420 / 1000000 = 57.9\,kNm$$

$$a_w = \frac{A - 2bt}{A} = \frac{3364 - 2 \cdot 120 \cdot 8}{3364} = 0.429 \le 0.5\,OK$$

$$M_{N,Rd} = M_{pl,Rd} \cdot \left(1 - \frac{N_{Ed}}{N_{pl,Rd}}\right) / \left(1 - \frac{A - 2bt}{2A}\right) = 57.9 \cdot \left(1 - \frac{1365}{1413}\right) / (1 - 0.429/2) = 57.9 \cdot 0.034 / 0.785 = 2.51\,kNm$$

The bending moment of Robot is at this member 5.13 kNm, so the utility ratio of the cross-section resistance is 5.13/2.51 = 2.05. Robot gave the utility ratio 2.96.

In this case the additional moment $qL^2/20$ = 1.64 kNm (see Table 3.10) given for this member in the optimiztion is not enough. The moment in Robot 5.13 kNm is about 3 times larger. It can be seen that when the axial force resistance is near the plastic axial resistance not much moment can be allowed to the member. The moment due to the bending of the entire truss is very much dependent on the height to span ratio of the truss, as above with the HEA trusses.

In practice the height to span ratio 1/20 is an extreme value. The cost ratio of SHS_24_20/SHS_24_10 is 1561/1217 = 1.28 (see Tables 3.10 and 3.9). However, the cost of the wall increases with the truss SHS_24_20 1.2 meters compared to the use of the truss SHS_24_10, meaning 1.2x24 = 28.8 m^2 wall. This means that if the wall unit cost is less than (1561-1217)/28.8 = 12 €/m^2, then it is more economical to use the truss SHS_24_20 instead of SHS_24_10. Typically the wall cost is larger.

4.3.7 SHS_36_10

Fig. 3.12 illustrates the optimal truss SHS_36_10. The Robot model of this truss is in *Fig.* 4.10.

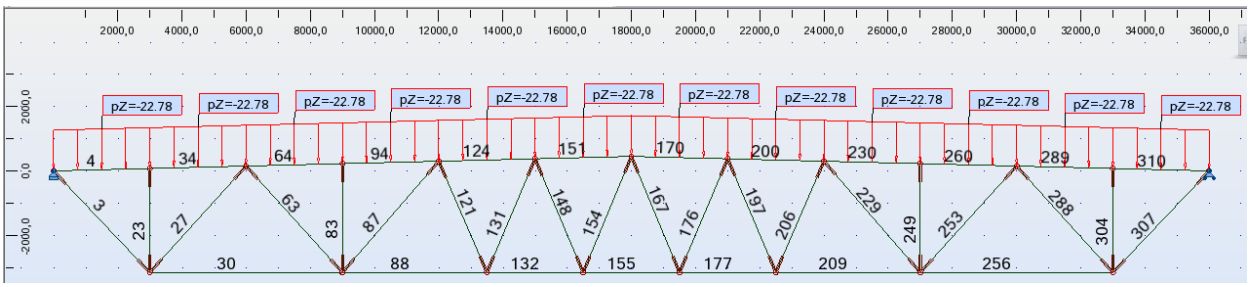

Figure 4.10. Robot model of SHS_36_10 at step 1.

The utility ratios of the members are shown in Table 4.8.

Table 4.8. Utility ratios of the members for SHS_36_10 at step 1.

Member	Section	Material	Lay (cm)	Laz (cm)	Ratio
3	RRHS 110x110x4	S355	90.91	101.01	0.88
4	RRHS 150x150x8	S420	47.28	52.53	0.44
23	RRHS 60x60x3	S355	125.96	139.95	1.05
27	RRHS 120x120x5	S355	86.26	95.85	0.98
30	RRHS 120x120x8	S420	120.30	133.67	0.44
34	RRHS 150x150x8	S420	47.28	52.53	0.46
63	RRHS 60x60x4	S355	177.75	197.50	0.96
64	RRHS 150x150x8	S420	47.28	52.53	0.81
83	RRHS 60x60x4	S355	134.51	149.46	0.78
87	RRHS 100x100x4	S355	105.65	117.39	0.98
88	RRHS 120x120x8	S420	90.23	100.25	0.68
94	RRHS 150x150x8	S420	47.28	52.53	0.78
121	RRHS 60x60x3	S355	146.93	163.25	0.36
124	RRHS 150x150x8	S420	47.28	52.53	0.90
131	RRHS 80x80x3	S355	110.45	122.72	0.71
132	RRHS 120x120x8	S420	60.15	66.83	0.72
148	RRHS 60x60x3	S355	149.62	166.24	0.04
151	RRHS 150x150x8	S420	47.28	52.53	0.91
154	RRHS 60x60x3	S355	152.32	169.24	0.21
155	RRHS 120x120x8	S420	60.15	66.83	0.73

4.3.7 SHS_36_20

Fig. 3.13 illustrates the optimal truss SHS_36_20. The Robot model of this truss is in *Fig.* 4.11.

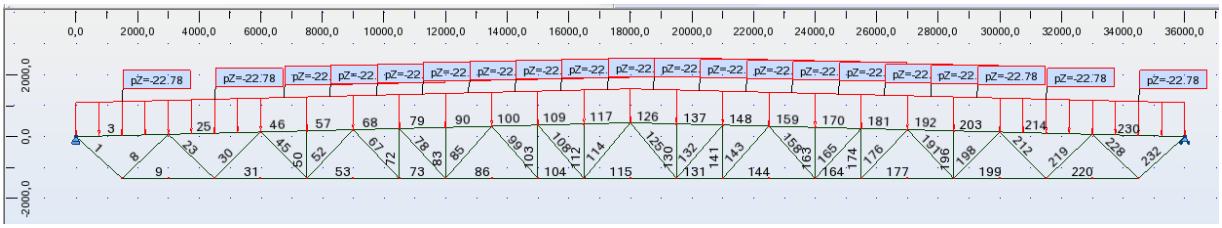

Figure 4.11. Robot model of SHS_36_20 at step 1.

The utility ratios of the members are shown in Table 4.9.

Table 4.9. Utility ratios of the members for SHS_36_20 at step 1.

Member	Section	Material	Lay (cm)	Laz (cm)	Ratio
1	RRHS 140x140x5	S355	33.18	36.87	0.60
3	RRHS 160x160x10	S420	44.88	49.86	0.36
8	RRHS 100x100x5	S355	48.52	53.91	1.00
9	RRHS 150x150x10	S420	48.21	53.56	0.36
23	RRHS 70x70x5	S355	71.15	79.06	0.91
25	RRHS 160x160x10	S420	44.88	49.86	0.73
30	RRHS 100x100x4	S355	49.02	54.47	0.90
31	RRHS 150x150x10	S420	48.21	53.56	0.62
45	SHS 60x60x5	S355	86.45	96.08	0.81
46	RRHS 160x160x10	S420	22.44	24.93	0.77
50	RRHS 60x60x3	S355	60.05	66.72	0.10
52	RRHS 90x90x3	S355	55.48	61.64	0.95
53	RRHS 150x150x10	S420	48.21	53.56	0.80
57	RRHS 160x160x10	S420	22.44	24.93	0.77
67	RRHS 60x60x3	S355	84.95	94.39	0.78
68	RRHS 160x160x10	S420	22.44	24.93	0.92
72	RRHS 60x60x3	S355	62.98	69.98	0.76
73	RRHS 150x150x10	S420	24.10	26.78	0.85
78	RRHS 60x60x3	S355	86.01	95.57	0.60
79	RRHS 160x160x10	S420	22.44	24.93	0.99

83	RRHS 60x60x3	S355	64.44	71.60	0.22
85	RRHS 60x60x3	S355	88.18	97.98	0.83
86	RRHS 150x150x10	S420	48.21	53.56	1.07
90	RRHS 160x160x10	S420	22.44	24.93	0.97
99	RRHS 60x60x3	S355	88.18	97.98	0.19
100	RRHS 160x160x10	S420	22.44	24.93	1.01
103	RRHS 60x60x3	S355	67.37	74.86	0.21
104	RRHS 150x150x10	S420	24.10	26.78	0.94
108	RRHS 60x60x3	S355	89.28	99.20	0.02
109	RRHS 160x160x10	S420	22.44	24.93	1.02
112	RRHS 60x60x3	S355	68.84	76.49	0.15
114	RRHS 60x60x3	S355	91.51	101.68	0.14
115	RRHS 150x150x10	S420	48.21	53.56	0.93
117	RRHS 160x160x10	S420	22.44	24.93	0.99

In this case the utility of the member 86 is 1.07 due to the moment resistance including axial force. The moment $qL^2/20$ = 10.25 kNm in optimization. The moment in Robot is 11.7 kNm, so the moment in optimizaton is a little bit too small. The ratio of these in 11.7/10.25 = 1.14 and the safe moment in optimization is $qL^2/17$.

4.3.8 Summary of step 1

If the truss can be designed without eccentricities at the joints, then the traditional truss analysis give safe values for the members, provided that additional moments are given to the chords. Safe values in the cases considered are $qL^2/10$ to the top chord and $qL^2/17$ for the bottom chord, except for the truss SHS_24_20. The height to span ration should be larger than 1/20. This additional moment is extremely important for slender trusses, say height to span ratio near by 1/20, then the moment due to deflection of the entire truss is about the same magnitude than the moment at the top chord due to continuous load at the top chord. In most of the cases the axial forces of the members are on the safe side using the traditional truss analysis compared to the results of the frame analysis, but not for at all members.

4.4 Step 2

4.4.1 HEA_24_10

Fig. 4.12 shows the Robot model of the truss HEA_24_10 at the step 2.

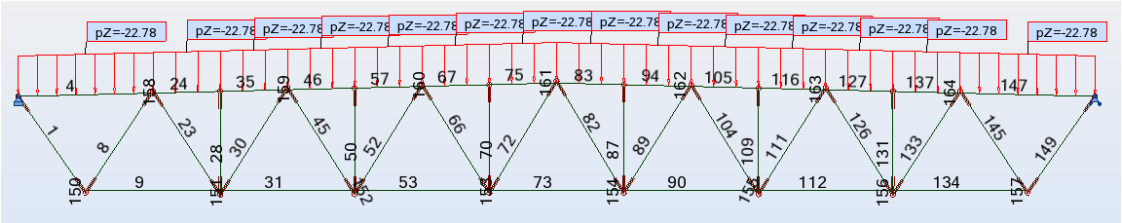

Figure 4.12. Robot model of HEA_24_10 at step 2.

In this frame model short eccentricity elements (members 150-164) can be seen at each joint. These member are modeled with HEM500 properties and their lengths and locations are as given *Fig.* 4.2. For HEA trusses the constant gap 40 mm was used. The bending moment diagram for this case is shown in *Fig*. 4.13.

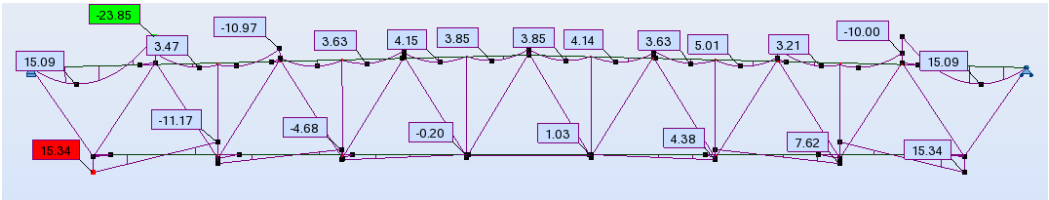

Figure 4.13. Bending moment diagram of truss HEA_24_20 at step 2.

By comparing this to *Fig*. 4.5 it can be seen that the maximum moment at the top chord increses, but generally the moments of the top chord are smaller. Instead the moments of the bottom chord are much larger than in *Fig*. 4.5 especially near the ends of the bottom chord. The axial forces are small there and the utilities of the members are given in Table 4.10.

Table 4.10 Utility ratios of the members for HEA_24_10 at step 2.

Member	Section	Material	Lay (cm)	Laz (cm)	Ratio
1	PIPE_4	S355	120.05	133.38	0.97
4	HEB 100	S460	65.05	118.49	0.72
8	PIPE_7	S355	83.60	92.89	1.07
9	HEA 100	S460	66.57	119.50	0.54
23	PIPE_3	S355	124.34	138.16	0.85
24	HEB 100	S460	32.45	59.10	0.62
28	PIPE_2	S355	129.01	143.35	0.46
30	PIPE_6	S355	84.34	93.71	1.00
31	HEA 100	S460	66.58	119.50	0.56
35	HEB 100	S460	32.54	59.27	0.64
45	PIPE_2	S355	157.61	175.12	0.83
46	HEB 100	S460	32.46	59.13	0.66
50	PIPE_2	S355	132.73	147.48	0.72
52	PIPE_5	S355	100.91	112.12	0.73
53	HEA 100	S460	66.59	119.52	0.68
57	HEB 100	S460	32.52	59.24	0.70
66	PIPE_1	S355	236.05	262.28	0.36
67	HEB 100	S460	32.48	59.15	0.71
70	PIPE_2	S355	135.54	150.59	0.78
72	PIPE_1	S355	242.12	269.02	0.40

73	HEA 100	S460	66.55	119.46	0.70
75	HEB 100	S460	32.50	59.20	0.73

The utility ratios of the chords are bout the same as in Table 4.1 (without eccentricities). The utility of the member 8 is now 1.07 and in Table 4.2 it was 1.00. The axial force and the lengths of this member are:

- Member 8: Without eccentricities: N_{Ed} = 292 kN, L = 2642 mm;
- Member 8: With eccentricities: N_{Ed} = 302 kN, L = 2720 mm.

The differences of the axial forces and the lengths (=> buckling) cause the difference of the utility ratios.

4.4.2 HEA_24_20

Fig. 4.13b shows the Robot model of the truss HEA_24_20 at the step 2.

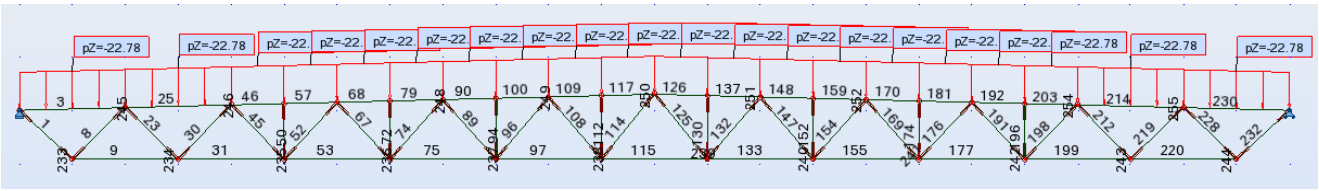

Figure 4.13b. Robot model of HEA_24_20 at step 2.

Table 4.11 Utility ratios of the members for HEA_24_20 at step 2.

Member	Section	Material	Lay (cm)	Laz (cm)	Ratio
1	PIPE_5	S355	49.15	49.15	0.76
3	HEB 120	S460	35.73	65.50	0.30
8	PIPE_5	S355	50.70	50.70	0.98
9	HEB 120	S460	35.70	58.90	0.34
23	PIPE_5	S355	50.89	50.89	0.56
25	HEB 120	S460	35.72	65.48	0.62
30	PIPE_6	S355	43.07	43.07	0.86
31	HEB 120	S460	35.70	58.90	0.58
45	PIPE_4	S355	66.11	66.11	0.64
46	HEB 120	S460	17.84	32.70	0.76
50	PIPE_1	S355	86.97	86.97	0.24
52	PIPE_4	S355	67.17	67.17	0.93
53	HEB 120	S460	35.71	58.91	0.74
57	HEB 120	S460	17.86	32.74	0.76
67	PIPE_3	S355	83.93	83.93	0.62
68	HEB 120	S460	17.86	32.74	0.92
72	PIPE_1	S355	90.94	90.94	0.15
74	PIPE_4	S355	68.70	68.70	0.58
75	HEB 120	S460	35.70	58.90	0.84
79	HEB 120	S460	17.85	32.73	0.92
89	PIPE_1	S355	124.22	124.22	0.48
90	HEB 120	S460	17.86	32.74	0.98
94	PIPE_1	S355	94.44	94.44	0.24

96	PIPE_2	S355	85.64	85.64	0.51
97	HEB 120	S460	35.71	58.92	0.88
100	HEB 120	S460	17.85	32.73	1.00
108	PIPE_1	S355	126.93	126.93	0.14
109	HEB 120	S460	17.86	32.75	1.00
112	PIPE_1	S355	98.36	98.36	0.22
114	PIPE_1	S355	131.10	131.10	0.16
115	HEB 120	S460	35.68	58.87	0.87
117	HEB 120	S460	17.86	32.74	0.99

The maximum utilities are near by 1.00 in this case.

4.4.3 HEA_36_10

Fig. 4.14 shows the Robot model of the truss HEA_36_10 at the step 2.

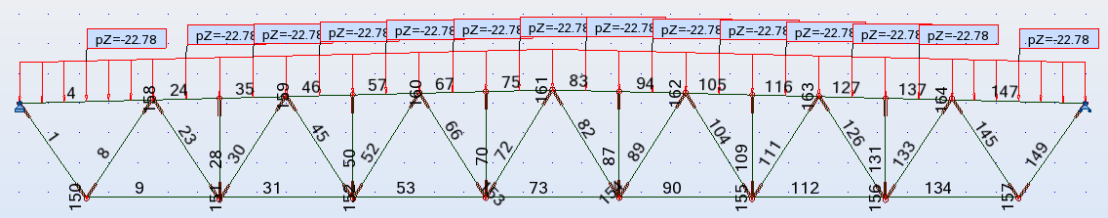

Figure 4.14. Robot model of HEA_36_10 at step 2.

Table 4.12 Utility ratios of the members for HEA_36_10 at step 2.

Member	Section	Material	Lay	Laz	Ratio
1	PIPE_4	S355	142.24	158.04	0.91
4	HEA 160	S460	61.71	113.04	0.73
8	PIPE_8	S355	77.26	85.84	0.90
9	HEA 140	S460	70.62	127.82	0.55
23	PIPE_5	S355	122.72	136.36	0.83
24	HEA 160	S460	30.80	56.42	0.72
28	PIPE_3	S355	157.03	174.48	0.43
30	PIPE_7	S355	86.96	96.62	0.87
31	HEA 140	S460	70.62	127.83	0.63
35	HEA 160	S460	30.85	56.51	0.66
45	PIPE_2	S355	237.55	263.95	0.93
46	HEA 160	S460	30.82	56.46	0.75
50	PIPE_3	S355	160.90	178.78	0.73
52	PIPE_6	S355	109.74	121.94	1.01
53	HEA 140	S460	70.62	127.83	0.77
57	HEA 160	S460	30.84	56.49	0.75
66	PIPE_1	S355	348.67	387.42	0.51
67	HEA 160	S460	30.83	56.48	0.81
70	PIPE_3	S355	164.39	182.66	0.76
72	PIPE_9	S355	276.57	307.29	0.71
73	HEA 140	S460	70.61	127.81	0.79
75	HEA 160	S460	30.84	56.49	0.79

4.4.4 HEA_36_20

Fig. 4.15 shows the Robot model of the truss HEA_36_20 at the step 2.

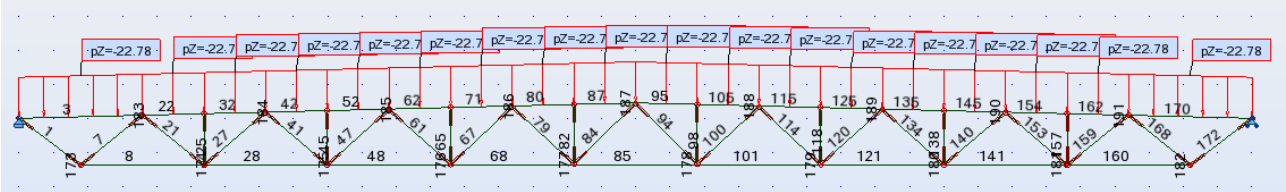

Figure 4.15. Robot model of HEA_36_20 at step 2.

Table 4.13 Utility ratios of the members for HEA_36_20 at step 2.

Member	Section	Material	Lay	Laz	Ratio
1	PIPE_8	S355	53.05	53.05	0.84
3	HEB 160	S460	47.83	88.96	0.39
7	PIPE_9	S460	43.80	43.80	0.80
8	HEB 160	S460	47.80	80.02	0.37
21	PIPE_5	S355	84.30	84.30	0.85
22	HEB 160	S460	23.90	44.46	0.64
25	PIPE_2	S355	84.19	84.19	0.20
27	PIPE_7	S355	58.42	58.42	0.96
28	HEB 160	S460	47.80	80.03	0.62
32	HEB 160	S460	23.90	44.46	0.61
41	PIPE_4	S355	108.41	108.41	0.86
42	HEB 160	S460	23.92	44.49	0.82
45	PIPE_2	S355	88.75	88.75	0.29
47	PIPE_6	S355	72.31	72.31	1.03
48	HEB 160	S460	47.80	80.02	0.77
52	HEB 160	S460	23.90	44.45	0.83
61	PIPE_2	S355	135.09	135.09	0.80
62	HEB 160	S460	23.92	44.50	0.94
65	PIPE_2	S355	93.18	93.18	0.33
67	PIPE_3	S355	110.95	110.95	1.07
68	HEB 160	S460	47.81	80.03	0.83
71	HEB 160	S460	23.89	44.43	0.96
79	PIPE_1	S355	203.65	203.65	0.04
80	HEB 160	S460	23.93	44.52	0.98
82	PIPE_2	S355	97.58	97.58	0.33
84	PIPE_1	S355	209.39	209.39	0.23
85	HEB 160	S460	47.81	80.03	0.82
87	HEB 160	S460	23.91	44.47	0.96

The utility ratio of the member 67 is now 1.07 and without eccentricities it was 1.03. The difference is due to the longer buckling length in this model.

4.4.5 SHS_24_10

Fig. 4.16 shows the Robot model of the truss SHS_24_10 at the step 2.

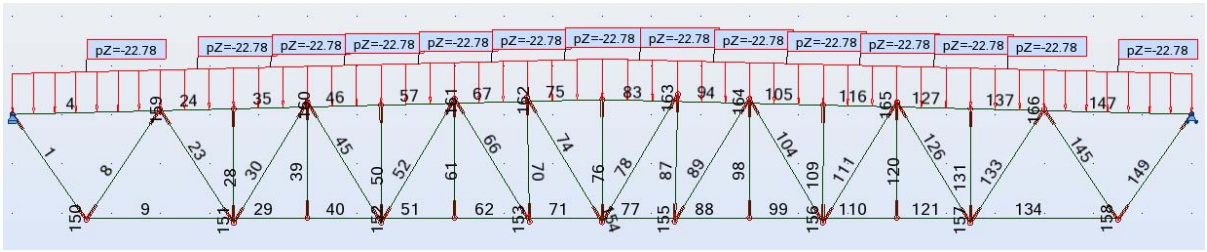

Figure 4.16. Robot model of SHS_24_10 at step 2.

Table 4.14 Utility ratios of the members for SHS_24_10 at step 2.

Member	Section	Material	Lay (cm)	Laz (cm)	Ratio
1	RRHS 90x90x3	S355	66.69	74.10	0.82
4	RRHS 110x110x6	S420	64.22	71.35	0.85
8	RRHS 100x100x3	S355	61.64	68.49	1.03
9	RRHS 100x100x5	S420	70.39	78.21	0.70
23	RHS 50x50x4	S355	133.98	148.92	0.85
24	RRHS 110x110x6	S420	32.05	35.62	0.87
28	RHS 40x40x3	S355	140.19	155.78	0.48
29	RRHS 100x100x5	S420	35.12	39.03	1.09
30	RRHS 80x80x3	S355	83.01	92.23	1.10
35	RRHS 110x110x6	S420	32.17	35.74	0.88
39	RHS 40x40x3	S355	142.15	157.95	0.04
40	RRHS 100x100x5	S420	35.19	39.10	0.71
45	RHS 40x40x3	S355	173.67	192.98	0.85
46	RRHS 110x110x6	S420	32.01	35.57	0.86
50	RHS 40x40x3	S355	144.21	160.25	0.92
51	RRHS 100x100x5	S420	35.16	39.07	1.54
52	RRHS 60x60x3	S355	114.29	126.99	1.15
57	RRHS 110x110x6	S420	32.14	35.71	0.88
61	RHS 40x40x3	S355	146.19	162.45	0.04
62	RRHS 100x100x5	S420	35.72	39.69	0.86
66	RHS	S355	176.62	196.26	0.27

	40x40x3				
67	RRHS 110x110x6	S420	31.56	35.07	0.88
70	RHS 40x40x3	S355	152.19	169.12	1.14
71	RRHS 100x100x5	S420	34.65	38.50	0.88
74	RHS 40x40x3	S355	178.93	198.83	0.02
75	RRHS 110x110x6	S420	32.57	36.19	0.87
76	RHS 40x40x3	S355	150.51	167.24	0.11

The utilities larger than 1.0 at the braces are mainly due to increased buckling lengths due to eccentricities. The large utilities of the bottom chord members 29 and 51 are due to interaction between axial force and moment of the cross-section resistance. *Fig.* 4.17 illustates the bending moment diagram of this truss.

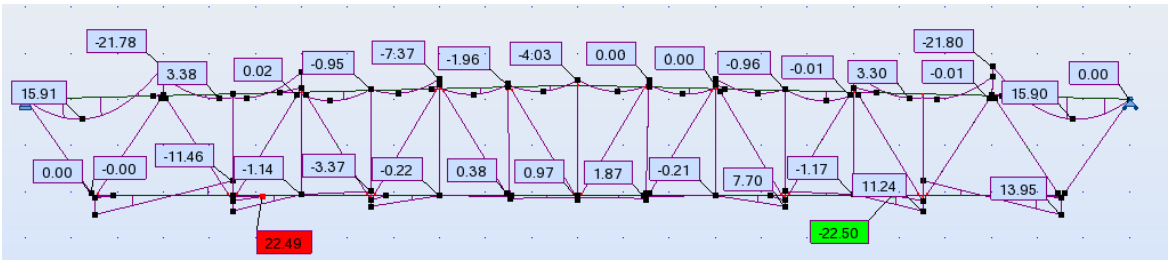

Figure 4.17. Bending moment diagram of truss SHS_24_10 at step 2.

It can be seen that there are rather large moments (member 29: 11.03 kNm, member 51: 7.69 kNm, numbers are not shown in *Fig*. 4.17) at the critical members. The member 51 is nearer the mid point of the truss so there is larger axial force than at the member 29, and larger utility ratio. Based on this it is recommended to avoid the eccentricities near the mid span of the truss. The eccentricity moments are larger near the ends of the bottom chord, but the utility ratios are small there, because the axial force is small. In optimization the additional moments at these members were 2.56 kNm, so basically the results of the optimization can be used only for the trusses which will be designed without eccentricities at the joints.

At the ends of the members 29 and 51 are gap KT-joints. This joint means almost always large eccentricity at the joint. The large eccentricity is avoided in practice using the joint layout presented in *Fig.* 4.18, although there exist no design method for this joint in the Eurocodes.

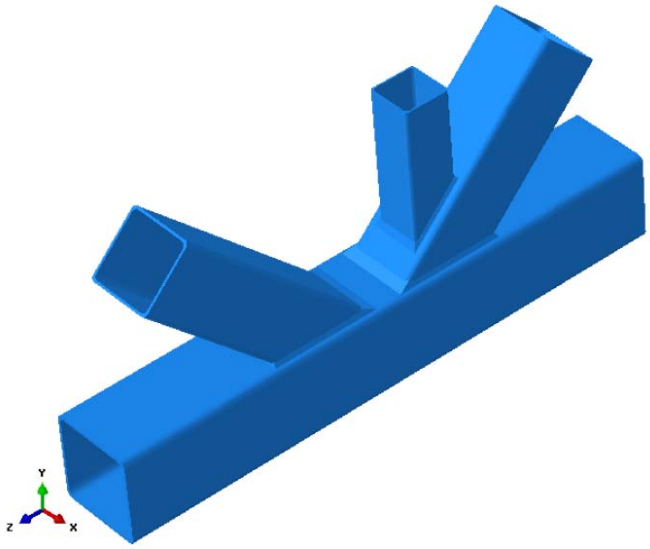

Figure 4.18. KT-joint made by welding the verctical to the tension diagonal.

4.4.6 SHS_24_20

Fig. 4.19 shows the Robot model of the truss SHS_24_20 at the step 2.

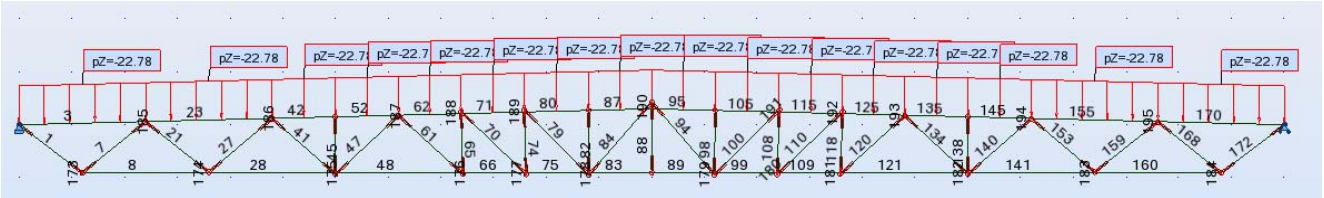

Figure 4.19. Robot model of SHS_24_20 at step 2.

Table 4.15 Utility ratios of the members for SHS_24_20 at step 2.

Member	Section	Material	Lay (cm)	Laz (cm)	Ratio
1	RRHS 110x110x4	S355	31.45	34.94	0.69
3	SHS 120x120x10	S420	49.36	54.85	0.41
7	RRHS 90x90x4	S355	39.65	44.06	0.94
8	RRHS 120x120x8	S420	48.11	53.46	0.44
21	RHS 50x50x5	S355	76.52	85.04	0.91
23	SHS 120x120x10	S420	49.40	54.89	0.86
27	RRHS 80x80x3	S355	45.19	50.22	0.96
28	RRHS 120x120x8	S420	48.14	53.49	0.73
41	RRHS 50x50x3	S355	75.56	83.96	0.91
42	SHS	S420	24.68	27.42	0.81

	120x120x10				
45	RRHS 50x50x3	S355	51.28	56.98	0.12
47	RHS 50x50x4	S355	79.18	88.01	1.04
48	RRHS 120x120x8	S420	48.47	53.86	1.31
52	SHS 120x120x10	S420	24.67	27.41	0.84
61	RRHS 50x50x3	S355	77.91	86.57	0.49
62	SHS 120x120x10	S420	24.33	27.03	0.92
65	RRHS 50x50x3	S355	55.79	61.98	0.40
66	RRHS 120x120x8	S420	24.08	26.75	1.38
70	RRHS 50x50x3	S355	81.00	90.00	0.27
71	SHS 120x120x10	S420	24.68	27.42	0.98
74	RRHS 50x50x3	S355	57.59	63.99	0.26
75	RRHS 120x120x8	S420	23.77	26.41	3.29
79	RRHS 50x50x3	S355	82.14	91.27	0.05
80	SHS 120x120x10	S420	25.08	27.87	0.98
82	RRHS 50x50x3	S355	57.65	64.05	0.15
83	RRHS 120x120x8	S420	23.97	26.63	2.23
84	RRHS 50x50x3	S355	86.19	95.76	0.10
87	SHS 120x120x10	S420	24.69	27.43	0.95
88	RRHS 50x50x3	S355	62.75	69.72	0.02

The large utilitities at the bottom chord are originating from the cross-section resistance for the axial force and the moment. In Fig. 4.20 is shown the bending moment diagram for this truss.

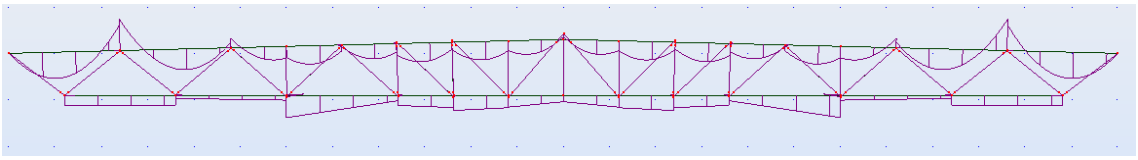

Figure 4.20. Bending moment diagram for the truss SHS_24_20 at step 2.

4.4.7 SHS_36_10

Fig. 4.21 shows the Robot model of the truss SHS_36_10 at the step 2.

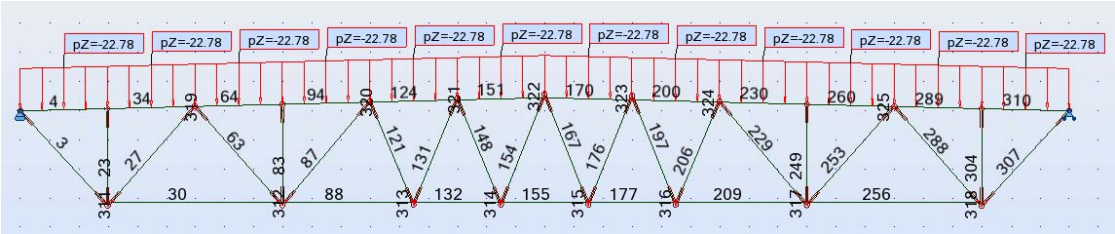

Figure 4.21. Robot model of SHS_36_10 at step 2.

Table 4.16 Utility ratios of the members for SHS_36_10 at step 2.

Member	Section	Material	Lay (cm)	Laz (cm)	Ratio
3	RRHS 110x110x4	S355	92.55	102.84	0.87
4	RRHS 150x150x8	S420	47.28	52.53	0.41
23	RRHS 60x60x3	S355	130.00	144.45	1.03
27	RRHS 120x120x5	S355	87.86	97.62	0.94
30	SHS 120x120x10	S420	123.39	137.10	1.09
34	RRHS 150x150x8	S420	47.28	52.54	0.44
63	RRHS 60x60x4	S355	180.58	200.64	1.03
64	RRHS 150x150x8	S420	47.27	52.52	0.71
83	RRHS 60x60x4	S355	137.78	153.09	0.77
87	RRHS 100x100x4	S355	107.66	119.62	0.92
88	SHS 120x120x10	S420	92.53	102.81	0.56
94	RRHS 150x150x8	S420	47.39	52.65	0.77
121	RRHS 60x60x3	S355	150.10	166.78	0.36
124	RRHS 150x150x8	S420	47.19	52.44	0.82
131	RRHS 80x80x3	S355	113.82	126.47	0.71
132	SHS 120x120x10	S420	61.71	68.56	0.60
148	RRHS 60x60x3	S355	154.06	171.17	0.05
151	RRHS 150x150x8	S420	47.24	52.49	0.86
154	RRHS 60x60x3	S355	158.66	176.29	0.22
155	SHS 120x120x10	S420	61.69	68.55	0.60

Now there are no KT-joints at the mid part of the truss and eccentricity moments are small there. Instead near the end of the bottom chord is large utility ratio (1.09) at the member 30. The reason for this can be seen in the bending moment diagram in *Fig.* 4.22.

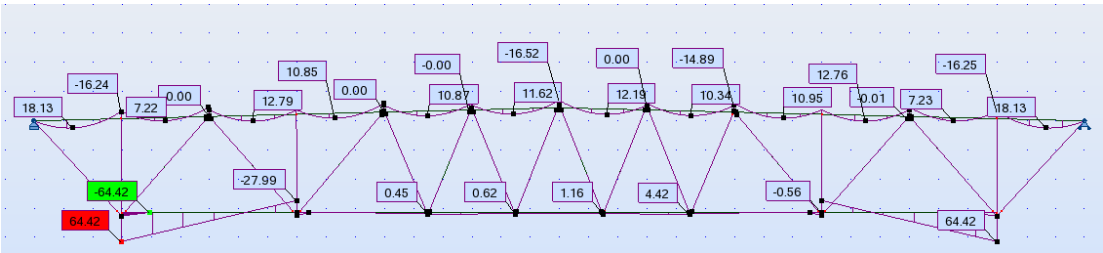

Figure 4.22. Bending moment diagram of the truss SHS_24_20 at the step 2.

The first joint at the end of the bottom chord should be designed so that the eccentricity is small.

4.4.8 SHS_36_20

Fig. 4.23 shows the Robot model of the truss SHS_36_20 at the step 2.

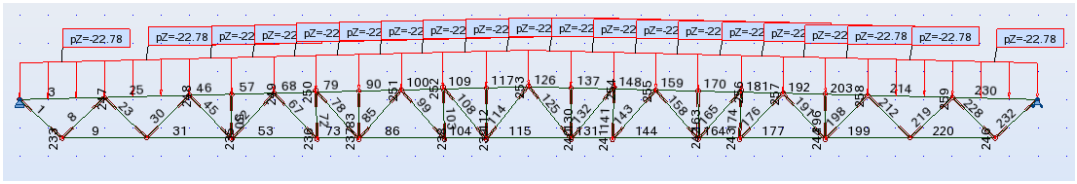

Figure 4.23. Robot model of SHS_36_20 at step 2.

Table 4.17 Utility ratios of the members for SHS_36_20 at step 2.

Member	Section	Material	Lay (cm)	Laz (cm)	Ratio
1	RRHS 140x140x5	S355	33.34	37.05	0.59
3	RRHS 160x160x10	S420	44.87	49.86	0.35
8	RRHS 100x100x5	S355	48.69	54.09	1.01
9	RRHS 150x150x10	S420	48.20	53.56	0.36
23	RRHS 70x70x5	S355	71.08	78.99	0.92
25	RRHS 160x160x10	S420	44.90	49.88	0.74
30	RRHS 100x100x4	S355	49.00	54.44	0.91
31	RRHS 150x150x10	S420	48.22	53.58	0.62
45	SHS 60x60x5	S355	88.01	97.81	0.80
46	RRHS 160x160x10	S420	22.43	24.92	0.76
50	RRHS 60x60x3	S355	62.14	69.05	0.11

52	RRHS 90x90x3	S355	56.38	62.64	0.97
53	RRHS 150x150x10	S420	48.62	54.02	0.79
57	RRHS 160x160x10	S420	22.43	24.92	0.77
67	RRHS 60x60x3	S355	87.07	96.74	0.82
68	RRHS 160x160x10	S420	22.05	24.50	0.90
72	RRHS 60x60x3	S355	67.50	75.00	0.83
73	RRHS 150x150x10	S420	23.68	26.31	0.85
78	RRHS 60x60x3	S355	89.90	99.89	0.62
79	RRHS 160x160x10	S420	22.84	25.37	1.01
83	RRHS 60x60x3	S355	66.41	73.79	0.24
85	RRHS 60x60x3	S355	89.49	99.43	0.85
86	RRHS 150x150x10	S420	48.67	54.07	1.46
90	RRHS 160x160x10	S420	22.43	24.92	0.97
99	RRHS 60x60x3	S355	90.70	100.78	0.21
100	RRHS 160x160x10	S420	22.02	24.47	1.00
103	RRHS 60x60x3	S355	72.57	80.63	0.22
104	RRHS 150x150x10	S420	23.66	26.29	0.94
108	RRHS 60x60x3	S355	93.90	104.33	0.03
109	RRHS 160x160x10	S420	22.86	25.40	1.02
112	RRHS 60x60x3	S355	71.15	79.05	0.16
114	RRHS 60x60x3	S355	94.15	104.61	0.14
115	RRHS 150x150x10	S420	48.18	53.53	0.93
117	RRHS 160x160x10	S420	22.44	24.93	0.99

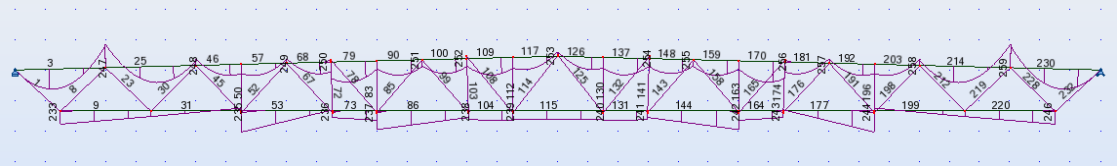

Figure 4.24. Bending moment of truss SHS_36_10 at the step 2.

The maximum utility is at the member 86 (utility 1.46) although eg. at the member 53 the utility is 0.79 and there is larger moment, but smaller axial load.

4.4.9 Summary of step 2, resistances of chords

After step 2 can be done the summary of the resistances of the chords, because the chord design is on the safe side at the step 2. This is due to fact, that the eccentricity moment are distributed only to the chords, and the eccentricity moments were taken into account at all joints, not considering the (corrected) rule of the clause 5.1.5(7) of EN 1993-1-8. The design of the top chord is OK when using the traditional truss analysis provided that the additional moment $qL^2/10$ is given to all members when checking the resistances of the top chords. The additional moments of the bottom chord cannot be estimated in forehand if large eccentricities are allowed at the joints. KT-joints should be avoided in the gap joints and eccentricity at the first joint of the bottom chord should be small. Instead of KT-joint the joint shown in *Fig*. 4.18 is recommended to be used.

4.4.10 Joint resistances at step 2

The numbering of joints in HEA trusses is shown in Fig. 4.25.

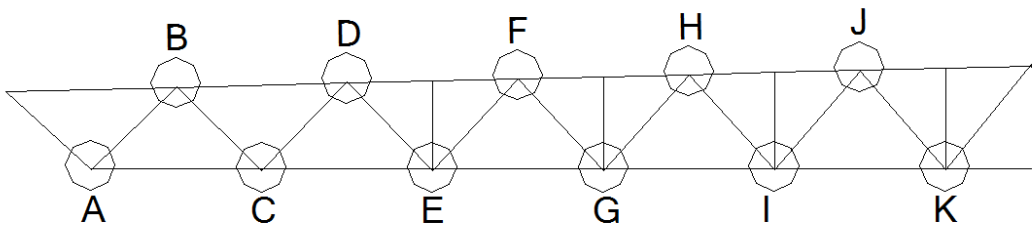

Figure 4.25. Numbering of joints in HEA trusses.

The utility ratios of the joints are given in Table 4.18.

Table 4.18. Utility ratios of joints of HEA trusses.

	HEA_24_10	HEA_24_20	HEA_36_10	HEA_36_20
Joint A	1,05 (1	0,96	1,20 (3	1,39
Joint B	0,79 (2	0,93	1.19	1,34
Joint C	0,98	0,91	1.32	0,87
Joint D	0,83	0,91	0,93	0,86
Joint E	0,83	0,73	0,77	0,86
Joint F	0,63	0,86	0,58	0,88
Joint G	0,76	0,81	0,68	0,88
Joint H	-	0,87	-	0,83
Joint I	-	0,96	-	0,92
Joint J	-	0,88	-	-
Joint K	-	0,12	-	-

1) Utility ratio of the chord shear failure: 1.39. After that largest utility ratio shown in table.
2) Utility ratio of the chord shear failure: 1.40. After that largest utility ratio shown in table.
3) Utility ratio of the chord shear failure: 1.56. After that largest utility ratio shown in table.

The chord shear failure with HEA/HEB members can be prevented at joints by additional web plates at the joints, locally. This may be more economical than to enlarge the entire chord.

The proportional eccentricties e/h_0 are given in Table 4.19.

Table 4.19. Eccentricities e/h_0 of HEA trusses.

	HEA_24_10	HEA_24_20	HEA_36_10	HEA_36_20
Joint A	0,48	0,08	0,41	0,10
Joint B	0,49	0,09	0,36	0,04
Joint C	0,92	0,13	0,80	0,10
Joint D	0,46	0,10	0,22	-0,04
Joint E	0,83	0,16	0,59	0,05
Joint F	0,35	0,00	0,10	-0,09
Joint G	0,57	0,15	0,32	-0,02
Joint H		-0,02		-0,16
Joint I		0,09		-0,09
Joint J		-0,04		
Joint K		0,07		

The eccentricities of the joints in the trusses HEA_24_20 and HEA_36_20 are within the limits $-0.55 \leq e/h_0 \leq 0.25$ of the clause 5.1.5(5) of EN 1993-1-8, so their design can be completed at this step. All joints of the truss HEA_24_10 are outside the limits and most of the joints of the truss HEA_36_10.

The numbering of the joints in SHS trusses is shown in Fig. 4.26.

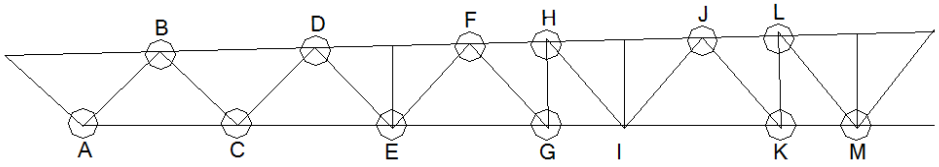

Figure 4.26. Numbering of joints in SHS trusses.

The utility ratios of the joints are given in Table 4.20.

Table 4.20. Utility ratios of joints of SHS trusses.

	SHS_24_10	SHS_24_20	SHS_36_10	SHS_36_20
Joint A	0,96 (1	0,79	0.84 (6	0,80
Joint B	0,89 (2	0,84	0,98	0,87
Joint C	0,95 (3	0,84	0,98	0,87
Joint D	0,89 (4	0,86	0,60	0,75
Joint E	0,89 (5	0.91 (7	0,79	0.87 (8

Joint F	0,75	0,84	0,63	0,84
Joint G	0,96	1.00	0,81	0,95
Joint H	0,76	0,88	-	0,89 (9
Joint I	0,98	1,05 (10	-	0,98
Joint J	-	0,90	-	0,96
Joint K	-	1,08 (10	-	1,03 (10
Joint L	-	-	-	0,92
Joint M	-	-	-	1,02 (10

1) Utility ratio of the chord face yield: 1.16. After that largest utility ratio shown in table.
2) Utility ratio of the chord face yield: 1.09. After that largest utility ratio shown in table.
3) Utility ratio of the chord face yield: 10.68. After that largest utility ratio shown in table.
4) Utility ratio of the chord face yield: 2.43. After that largest utility ratio shown in table.
5) Utility ratio of the chord face yield: 4.03. After that largest utility ratio shown in table.
6) Utility ratio of the chord face yield: 1.63. After that largest utility ratio shown in table.
7) Utility ratio of the chord face yield: 1.42. After that largest utility ratio shown in table.
8) Utility ratio of the chord face yield: 1.21. After that largest utility ratio shown in table.
9) Utility ratio of the chord face yield: 1.04. After that largest utility ratio shown in table.
10) Shear and axial force resistance at the gap.

The proportional eccentricties e/h_0 are given in Table 4.21.

Table 4.21. Eccentricities e/h_0 of SHS trusses.

	SHS_24_10	SHS_24_20	SHS_36_10	SHS_36_20
Joint A	0,41	0,06	0,86	0,09
Joint B	0,25	-0,04	0,07	-0,02
Joint C	1,06	-0,06	0,68	0,00
Joint D	0,92	-0,04	0,20	0,00
Joint E	0,98	0,26	0,51	0,36
Joint F	0,84	-0,09	0,44	-0,01
Joint G	0,70	0,25	0,48	0,35
Joint H	0,74	0,34	-	0,39
Joint I	0,81	0,29	-	0,34
Joint J	-	0,34	-	-0,04
Joint K	-	-	-	0,41
Joint L	-	-	-	0,45
Joint M	-	-	-	0,39

It can be seen that all trusses include joints where the eccentricity limits are exceeded, so the step 3 is essential. It can be noted that in K-joints the eccentricities are much smaller than in KT- and N-joints. Also, it can be noted that when the height to span ratio is 20 the eccentricities are much

smaller than when this ratio is 10. Especially large eccentricities can be noted at the truss SHS_24_10. The same can be found in HEA trusses. It is excepted that the large eccentricities have considerable effect to the brace and joint design.

4.5 Step 3

4.5.1 Utilities of braces and joints

The resistances of the chord have been completed in step 2. At this step the resistance of the braces and joints should be checked by distributing the eccentricity moments of the joints to all members of the joint, and the axial forces of the joints are increased by the formula proposed in (Wardenier, 1984):

$$N_{Ed,new} = N_{Ed} + A \cdot \frac{M_{ecc}}{W} \tag{4.2}$$

where

- N_{Ed} is the axial force of the brace from the frame model;
- A is the area of the brace;
- M_{ecc} is the part of the eccentricity moment of the brace;
- W is the elastic modulus of the brace.

The utility ratios of the braces with eccentricity moments are given in Table 4.22 for HEA_24_10 and HEA_36_10 trusses. HEA_24_20 and HEA_36_20 need not to be considered, because the eccentricity limits were OK.

Table 4.22. Utility ratios of braces for HEA trusses with eccentricity moments.

	HEA_24_10	HEA_36_10
1st brace	1,24	1,04
2nd brace	2,06	1,85
3rd brace	0,91	0,60
4th brace	0,57	0,34
5th brace	2,14	2,84
6th brace	0,89	0,96
7th brace	0,79	0,72
8th brace	1,39	2,38
9th brace	0,36	0,51
10th brace	0,79	0,76
11th brace	0,42	0,68

The utility ratios of the joints of HEA trusses are given in Table 4.23 with additions from the eccentricity moments based on Eq. (2).

Table 4.23. Utility ratios of joints of HEA trusses with eccentricity moments.

	HEA_24_10	HEA_36_10

Joint A	1,48 (1	2,04 (4
Joint B	0,88 (2	1,31 (5
Joint C	1,30 (3	1,73
Joint D	0,86	1,08
Joint E	0,91	0,81
Joint F	0,63	0,58
Joint G	0,76	0,68

1) Utility ratio of the chord shear failure: 2.44. After that largest utility ratio shown in table.
2) Utility ratio of the chord shear failure: 1.42. After that largest utility ratio shown in table.
3) Utility ratio of the chord shear failure: 1.38. After that largest utility ratio shown in table.
4) Utility ratio of the chord shear failure: 2.65. After that largest utility ratio shown in table.
5) Utility ratio of the chord shear failure: 1.37. After that largest utility ratio shown in table.

The utility ratios of the braces with eccentricity moments are given in Table 4.24 for SHS trusses.

Table 4.24. Utility ratios of braces for SHS trusses with eccentricity moments.

	SHS_24_10	SHS_24_20	SHS_36_10	SHS_36_20
1st brace	1,10	0,75	1,51	0,65
2nd brace	1,38	0,97	1,64	1,04
3rd brace	0,91	0,92	1,80	0,92
4th brace	0,41	0,99	1,15	0,91
5th brace	1,35	0,95	1,05	0,84
6th brace	0,10	0,11	1,30	0,15
7th brace	0,89	0,99	0,37	1,03
8th brace	0,98	0,50	0,84	0,82
9th brace	1,08	0,41	0,06	0,85
10th brace	0,06	0,27	0,25	0,63
11th brace	0,29	0,26	-	0,25
12th brace	0,99	0,05	-	0,86
13th brace	0,02	0,15	-	0,21
14th brace	0,11	0,10	-	0,22
15th brace	-	-	-	0,03
16th brace	-	-	-	0,16
17th brace	-	-	-	0,14

It can be seen that the utilities of the braces are very large, maximum 1.80, when the eccentricity is large at the joint of the brace, logically. This is especially true for the trusses with height to span ratio 10. If this ratio is 20 then the utilities are in maximum 1.04.

The utility ratios of the joints of SHS trusses are given in Table 4.25 with additions from the eccentricity moments based on Eq. (4.2).

Table 4.25. Utility ratios of joints of SHS trusses with eccentricity moments.

	SHS_24_10	SHS_24_20	SHS_36_10	SHS_36_20
Joint A	1.43 (1	0,86	1,72	0,94
Joint B	0.93 (2	0,82	0,99	0,87
Joint C	1.09 (3	0,82	0.98 (7	0,87
Joint D	0.94 (4	0,86	0,60	0,75
Joint E	0.95 (5	0.92 (8	0,79	0.87 (9
Joint F	0.75 (6	0,84	0,63	0,84
Joint G	1,00	1,00	0,81	0,97
Joint H	0,76	0,88	-	1,06
Joint I	0,98	1,05	-	0,98
Joint J	-	0,90	-	0,96
Joint K	-	1,08	-	1,03
Joint L	-	-	-	0,92
Joint M	-	-	-	1,02

1) Utility ratio of the chord face yield: 1.56. After that largest utility ratio shown in table.
2) Utility ratio of the chord face yield: 1.21. After that largest utility ratio shown in table.
3) Utility ratio of the chord face yield: 10.91. After that largest utility ratio shown in table.
4) Utility ratio of the chord face yield: 2.99. After that largest utility ratio shown in table.
5) Utility ratio of the chord face yield: 5.08. After that largest utility ratio shown in table.
6) Utility ratio of the chord face yield: 1.35. After that largest utility ratio shown in table.
7) Utility ratio of the chord face yield: 1.47. After that largest utility ratio shown in table.
8) Utility ratio of the chord face yield: 1.55. After that largest utility ratio shown in table.
9) Utility ratio of the chord face yield: 1.27. After that largest utility ratio shown in table.

In SHS trusses the utilities of the joints are large in many joints due to chord face yielding, if the eccentricty of the joint is large. Next critical failure mode is the shear and axial failure at the gap.

5. Conclusions

The purpose of this study was to provide a comprehensive evaluation of different types of member profiles in roof trusses. In the first part eight trusses were optimized using the topology optimization method of (Mela, 2013). After that, the basic research question was to evaluate, whether the trusses which were defined using the traditional truss analysis (see *Fig*. 4.1) in the optimization fulfill the requirements of the Eurocodes? The evaluation was done in three steps to report the effects at each step to the utility ratios of the members and joints. After the last step all requirements were checked. The results were as follows.

In step 1 frame analysis model was used for the optimized trusses. This model simulates the truss which is designed without eccentricities at the joints. The evaluation was done with the frame analysis where the chords were modeled as continuous beams. If the truss can be designed without eccentricities at the joints, then the raditional truss analysis is suitable for the design of the members, provided that the moment $qL^2/10$ is added to the top chord. The additional moment $qL^2/17$ to the bottom chord was enough in all cases, but not in the truss SHS_24_20. When the truss is slender, meaning height to span ratio 20, then the bending of the entire truss means moments to the bottom chord and the additional moment $qL^2/17$ may not be enough. With the ratio 10 this additional moment was suitbale in all cases. When the truss can be designed without eccentricties then the axial forces of the braces may increase in some cases, although in most of the cases they

decreased. This can be taken into account using the traditional truss analysis by increasing e.g. buckling length factors of the braces, say from 0.90 to 0.95.

If the truss is designed without eccentricties at the joints, then the overlapped joints should be used and they are more costly than gap joints. In this study only gap joints were considered, and the resistances of the joints were not checked at step 1.

In step 2 frame models were generated with the eccentricities at the joints (see *Fig.* 4.2). In HEA trusses the constant gap 40 mm was used and in SHS trusses the gap varied in the joints and the minimum gap based on EN 1993-1-8 (or at least 10 mm) was used at the joints.

After step 2 the summary of the resistances of the chords was done, because the chord design is on the safe side at the step 2. The design of the top chord was OK when using the traditional truss analysis provided that the additional moment $qL^2/10$ is given to all members when checking the resistances of the top chords. The additional moments of the bottom chord cannot be estimated in forehand if large eccentricities are allowed at the joints. The brace design was OK using a little bit larger buckling factor. One motivation for this was that the system lengths are little longer using eccentricties than without them.

KT-joints should be avoided in the gap joints and eccentricity at the first joint of the bottom chord should be small. Instead of KT-joint, the joint shown in *Fig*. 4.18 is recommended to be used to avoid large eccentricities.

The eccentricities of the joints in the trusses HEA_24_20 and HEA_36_20 were within the limits of Eurocodes, so their design could be completed at this step. All joints of the truss HEA_24_10 are outside the limits and most of the joints of the truss HEA_36_10. Local web strengthenings were required in some joints.

All SHS trusses included joints where the eccentricity limits were exceeded. It could be noted that in K-joints the eccentricities are much smaller than in KT- and N-joints. Also, it could be noted that when the height to span ratio is 20 the eccentricities are much smaller than when this ratio is 10. The same could be found in HEA trusses. The chord strenghtening was needed at some joints.

In step 3 the utilities of the braces and joints were checked by distributing the eccentricity moments to all members connected at the joints. The resistances of the braces were checked for the interaction of the axial force and the moment using Method B of EN 1993-1-1. The resistances of the joints were checked using the equations of EN 1993-1-8 by increasing the axial forces of the braces using Eq. (4.2).

Very large utility ratios, in maximum 1.80, were observed at the braces at this step. Also, the utilities of the joints were very large at the joints where the eccentricities were large, as expected.

Results of optimization. Based on this evaluation it can be conluded that the results of optimization can be compared with each other. Some braces should be larger but this does not increase the costs of the trusses considerably. Some joints need local stiffeners, but similar needs were both at the HEA and SHS trusses. Proposals for chord and brace design were given when the traditional truss analysis is used in optimization. Special care should be given when very slender trusses are

optimized with height to span ratio near 20. The bending of the entire truss causes additional moments to the bottom chord which can be as large as the moments of the top chord due to uniform load at the top chord. The resistance checks of the commercial programs should be used carefully. The completed study implies clearly, that the frame analysis including eccentricities should be implemented in the future to the optimization to get reliable solutions for the real projects. But, optimization can be used for comparing different solutions, as was done in this study. No bias was found when evaluating the results.

The final outcome in this study is:

- SHS trusses are 5–10 % more economical than HEA trusses.
- The weight of the minimum cost SHS trusses is 4–8 % greater, except for the 24 m span truss with $h = L/10$, where SHS truss is 6 % lighter than HEA truss.

SHS truss is made of cold-formed square hollow section members with S420 chords and S355 braces. HEA truss is made of hot-rolled HEA/HEB chords (S460) and cold-formed circular hollow section (S355) braces. Welded gap joints are used in both trusses.

Acknowledgement
Financial support of SSAB is gratefully acknowledged.